

This discussion paper is/has been under review for the journal Atmospheric Chemistry and Physics (ACP). Please refer to the corresponding final paper in ACP if available.

Explaining global surface aerosol number concentrations in terms of primary emissions and particle formation

D. V. Spracklen¹, K. S. Carslaw¹, J. Merikanto¹, G. W. Mann¹, S. Pickering¹,
J. A. Ogren², E. Andrews², U. Baltensperger³, E. Weingartner³, M. Boy⁴,
M. Kulmala⁴, L. Laakso⁴, H. Lihavainen⁵, N. Kivekäs⁵, N. Mihalopoulos⁶,
G. Kouvarakis⁶, S. G. Jennings⁷, W. Birmili⁸, A. Wiedensohler⁸, R. Weller⁹,
P. Laj¹⁰, K. Sellegrí¹¹, B. Bonn¹², and R. Krejci¹³

¹Institute for Climate and Atmospheric Science, School of Earth and Environment, University of Leeds, LS2 9JT, UK

²NOAA/ESRL Global Monitoring Division, 325 Broadway R/GMD1, Boulder, Co 80305, USA

³Paul Scherrer Institut, Laboratory of Atmospheric Chemistry, 5232 Villigen, Switzerland

⁴Department of Physical Sciences, University of Helsinki, Finland

⁵Climate Change, Finnish Meteorological Institute, Helsinki, Finland

⁶Department of Chemistry, University of Crete, University campus, P.O. Box 2208, 71003, Voutes, Heraklion, Crete, Greece

ACPD

9, 26377–26419, 2009

Explaining global aerosol number concentrations

D. V. Spracklen et al.

Title Page

Abstract

Introduction

Conclusions

References

Tables

Figures

◀

▶

◀

▶

Back

Close

Full Screen / Esc

Printer-friendly Version

Interactive Discussion



⁸ Leibniz Institute for Tropospheric Research, Permoserstrasse 15, 04318 Leipzig, Germany

⁹ Alfred Wegener Institute, Am Handelshafen 12, 27570 Bremerhaven

¹⁰ Laboratoire de Glaciologie et Géophysique de l'Environnement CNRS/Université Grenoble 1, Grenoble, France

¹¹ Laboratoire de Météorologie Physique, Université Clermont-Ferrand/CNRS, Clermont-Ferrand, France

¹² J.W. Goethe University, Inst. for Atmospheric and Environmental Sciences, Frankfurt/Main, Germany

¹³ Department of Applied Environmental Science (ITM), Stockholm University, 10691 Stockholm, Sweden

Received: 10 November 2009 – Accepted: 25 November 2009 – Published: 10 December 2009

Correspondence: D. V. Spracklen (dominick@env.leeds.ac.uk)

Explaining global aerosol number concentrations

D. V. Spracklen et al.

[Title Page](#)

[Abstract](#)

[Introduction](#)

[Conclusions](#)

[References](#)

[Tables](#)

[Figures](#)



[Back](#)

[Close](#)

[Full Screen / Esc](#)

[Printer-friendly Version](#)

[Interactive Discussion](#)



Abstract

ACPD

9, 26377–26419, 2009

We use observations of total particle number concentration at 36 worldwide sites and a global aerosol model to quantify the primary and secondary sources of particle number. We show that emissions of primary particles can reasonably reproduce the spatial pattern of observed condensation nuclei (CN) ($R^2=0.51$) but fail to explain the observed seasonal cycle at many sites ($R^2=0.1$). The modeled CN concentration in the free troposphere is biased low (normalised mean bias, NMB=−88%) unless a secondary source of particles is included, for example from binary homogeneous nucleation of sulfuric acid and water (NMB=−25%). Simulated CN concentrations in the continental boundary layer (BL) are also biased low (NMB=−74%) unless the number emission of anthropogenic primary particles is increased or an empirical BL particle formation mechanism based on sulfuric acid is used. We find that the seasonal CN cycle observed at continental BL sites is better simulated by including a BL particle formation mechanism ($R^2=0.3$) than by increasing the number emission from primary anthropogenic sources ($R^2=0.18$). Using sensitivity tests we derive optimum rate coefficients for this nucleation mechanism, which agree with values derived from detailed case studies at individual sites.

1 Introduction

There are two sources of particles in the atmosphere. Primary particles are emitted directly to the atmosphere and secondary particles are formed from gas-to-particle conversion. The relative contribution of these two sources to global aerosol is poorly understood, but it is important to quantify if we are to understand long-term aerosol trends and the impact of aerosol on climate. Here we use observations of total particle number concentration at sites around the world together with a global aerosol model to understand the sources of particle number.

Explaining global aerosol number concentrations

D. V. Spracklen et al.

[Title Page](#)

[Abstract](#)

[Introduction](#)

[Conclusions](#)

[References](#)

[Tables](#)

[Figures](#)

◀

▶

◀

▶

[Back](#)

[Close](#)

[Full Screen / Esc](#)

[Printer-friendly Version](#)

[Interactive Discussion](#)



Primary particles are emitted directly to the atmosphere, for example from biomass burning, combustion of fossil fuels and uplift of sea-spray and dust from the Earth's surface. Neither the emission strength nor the size distribution of primary particles is well known. A small uncertainty in the size distribution of primary particles (for a given mass) leads to large uncertainty in both the number emission and atmospheric number concentration of particles (Spracklen et al., 2005b).

Secondary particles formed from particle formation are observed at many surface locations around the world and also within the free and upper troposphere (Kulmala et al., 2004). Particle formation events are associated with a rapid increase in the number concentration of ultrafine particles followed by particle growth. Such events have been observed at sites ranging from Antarctica (Koponen et al., 2003), Arctic (Vehkamäki et al., 2004), boreal forest (Mäkelä et al., 1997; Kulmala et al., 1998b; Dal Maso et al., 2005), suburban and urban regions (Birmili and Wiedensohler, 2000; Gaydos et al., 2005) and coastal environments (O'Dowd et al., 1999). Several observations using multiple measurement stations have shown that formation events can occur more or less uniformly in air masses extending over hundreds of kilometres (Kulmala et al., 1998b, 2001; Vana et al., 2004; Komppula et al., 2006). Large concentrations of ultrafine (<20 nm) particles have also been observed in the free and upper troposphere (e.g., Clarke et al., 1998, 1999; Weingartner et al., 1999) and frequent new particle formation has now also been recorded at high altitudes (Venzac et al., 2008). The importance of secondary particle formation on a global scale is uncertain, though it may make a significant contribution to both global condensation nuclei (CN) (Spracklen et al., 2006) and cloud condensation nuclei (CCN) concentrations (Spracklen et al., 2008; Kuang et al., 2009; Makkonen et al., 2009; Pierce and Adams, 2009; Wang and Penner, 2009).

Despite such frequent occurrence in the atmosphere, and potential importance to global aerosol, the underlying mechanism of new particle formation is not known. Several mechanisms have been proposed including binary homogeneous nucleation (BHN) of $\text{H}_2\text{SO}_4\text{-H}_2\text{O}$ (Jaecker-Voirol and Mirabel, 1988; Kulmala et al., 1998a;

Explaining global aerosol number concentrations

D. V. Spracklen et al.

[Title Page](#)

[Abstract](#)

[Introduction](#)

[Conclusions](#)

[References](#)

[Tables](#)

[Figures](#)

◀

▶

◀

▶

[Back](#)

[Close](#)

[Full Screen / Esc](#)

[Printer-friendly Version](#)

[Interactive Discussion](#)



Vehkamäki et al., 2002), ternary nucleation (TN) of $\text{H}_2\text{SO}_4\text{-H}_2\text{O-NH}_3$ (Napari et al., 2002) and ion-induced nucleation (Modgil et al., 2005). BHN is strongly temperature dependent and only produces new particles in the cold free and upper troposphere (Weber et al., 1999; Adams and Seinfeld, 2002; Spracklen et al., 2005a; Lucas and Akimoto, 2006). Revised parameterizations of ternary nucleation (Yu, 2006; Anttila et al., 2005; Merikanto et al., 2007) also suggest that this mechanism is not a significant source of particles in the lower troposphere (Elleman and Covert, 2009). Neither of these mechanisms is therefore likely to explain particle formation observed in the boundary layer (BL). Ion-induced nucleation potentially contributes to both free troposphere (FT) and BL particle formation (Kazil et al., 2006; Yu et al., 2008). However, some studies (Kulmala et al., 2007; Boy et al., 2008) suggest that ion-induced nucleation contributes less than 10% of particle formation in the continental BL.

While our mechanistic understanding of nucleation remains so uncertain, an alternative approach has been used to explain observed particle formation and to estimate the impact of nucleation on global aerosol properties. Observations of surface particle formation events have been analysed to develop empirical particle formation mechanisms. The formation rate of molecular clusters (1 nm to 1.5 nm in diameter) is found to be proportional to the gas-phase sulfuric acid concentrations to the power 1 to 2 (Weber et al., 1996; Kulmala et al., 2006; Sihto et al., 2006; Riipinen et al., 2007; Kuang et al., 2008). The power one dependence of the cluster formation rate on sulfuric acid has been described in terms of an activation mechanism (Kulmala et al., 2006) where sulfuric acid particles are stabilized by a secondary species such as organics. A power two dependence has been explained by proposing a kinetic nucleation mechanism (McMurry and Friedlander, 1979).

Global aerosol microphysics models can now prognose CN and CCN concentrations for the first time (e.g., Adams and Seinfeld, 2002, 2003; Easter et al., 2004; Pierce and Adams, 2006; Pierce et al., 2007; Spracklen et al., 2005a,b; Stier et al., 2005) and are being used to understand the atmospheric processes controlling global aerosol. There is therefore an urgent need to evaluate these new models against observations. The

Explaining global aerosol number concentrations

D. V. Spracklen et al.

[Title Page](#)

[Abstract](#)

[Introduction](#)

[Conclusions](#)

[References](#)

[Tables](#)

[Figures](#)

◀

▶

◀

▶

[Back](#)

[Close](#)

[Full Screen / Esc](#)

[Printer-friendly Version](#)

[Interactive Discussion](#)



significant uncertainties associated both with the treatment of primary emissions and particle formation mean that model skill may be lacking. The size of primary particles emitted in global models must take into account the size distribution of the primary particles at the point of emission as well as the ageing that occurs at sub-model grid scales (Pierce et al., 2009). Because the mechanisms of atmospheric new particle formation are unknown there are also significant uncertainties in the global secondary particle formation rate (Spracklen et al., 2008).

Remote marine boundary layer (MBL) particle number size distributions can largely be explained by a combination of entrainment of particles from the FT (produced by particle formation in the upper troposphere) and primary sea-salt emissions, although there are significant regional discrepancies between model and observations (Easter et al., 2004; Spracklen et al., 2005a, 2007; Pierce and Adams, 2006; Trivitayanurak et al., 2008). Vertical profiles of CN over the remote MBL can also be explained by BHN (Spracklen et al., 2005a).

Simulated CN concentrations in the continental BL are greatly enhanced by primary sulfate (Adams and Seinfeld, 2002, 2003; Spracklen et al., 2005b; Wang et al., 2009), carbonaceous aerosol (Pierce et al., 2007) and BL particle formation (Spracklen et al., 2006, 2008; Makkonen et al., 2009; Chang et al., 2009). While Pierce and Adams (2009) show that observed CN at continental BL sites can be largely explained by primary emissions alone, other studies suggest a large contribution from particle formation (Spracklen et al., 2006, 2008; Makkonen et al., 2009).

In this study, we use observations of total particle number concentration together with a global aerosol model to better understand the contribution of particle formation and primary emissions to global aerosol number. We compile measurements of the total particle number concentration, reported for particle sizes larger than a few nanometers (typically 3–10 nm in diameter), from 36 surface sites around the world. Although such small particles are not directly relevant to climate, our dataset is the largest available for evaluating aerosol microphysics models and to understand the sources of global aerosol number. Furthermore, it is thought that subsequent growth

Explaining global aerosol number concentrations

D. V. Spracklen et al.

[Title Page](#)

[Abstract](#)

[Introduction](#)

[Conclusions](#)

[References](#)

[Tables](#)

[Figures](#)

◀

▶

◀

▶

[Back](#)

[Close](#)

[Full Screen / Esc](#)

[Printer-friendly Version](#)

[Interactive Discussion](#)



of these particles to larger sizes may contribute significantly to global concentrations of CCN (e.g., Spracklen et al., 2008; Kuang et al., 2009) making them indirectly important to climate.

2 Model Description

5 2.1 General

We use the GLOMAP aerosol microphysics model (Spracklen et al., 2005a,b), which is an extension of the TOMCAT 3-D global chemical transport model (Chipperfield, 2006) to simulate sulfate (SU), sea salt (SS), elemental carbon (EC) and organic carbon (OC) for the year 2000. Large-scale transport and meteorology is specified from 6-h European Centre for Medium-Range Weather Forecasts (ECMWF) analyses. We use a horizontal resolution of $\sim 2.8^\circ$ by $\sim 2.8^\circ$ and 31 vertical levels between the surface and 10 hPa.

GLOMAP treats the particle size distribution using either a two-moment modal (Manktelow et al., 2007) or a two-moment sectional (bin) (Spracklen et al., 2005a) scheme. Here we use the sectional scheme and treat two externally mixed distributions, each described with 20 sections spanning 3 nm to $10\ \mu\text{m}$ dry diameter. One distribution, representing freshly emitted primary carbonaceous aerosol, contains OC and EC, is treated as non-hydrophilic and is not wet scavenged. The other distribution contains SU, SS, EC and OC, is hydrophilic and is wet scavenged. Non-hydrophilic particles age to become hydrophilic through condensation of soluble gas-phase species and coagulation with hydrophilic particles. Total simulated particle number is the sum of particles in these two distributions. The microphysical processes in the model include nucleation, coagulation, condensation of gas-phase species, in-cloud and below-cloud aerosol scavenging and deposition, dry deposition and cloud processing.

Concentrations of OH, O_3 and NO_3 and HO_2 are specified using 6-h monthly mean 3-D concentrations from a TOMCAT simulation with detailed tropospheric chemistry

Explaining global aerosol number concentrations

D. V. Spracklen et al.

[Title Page](#)

[Abstract](#)

[Introduction](#)

[Conclusions](#)

[References](#)

[Tables](#)

[Figures](#)

◀

▶

◀

▶

[Back](#)

[Close](#)

[Full Screen / Esc](#)

[Printer-friendly Version](#)

[Interactive Discussion](#)



(Arnold et al., 2005). Concentrations of H₂O₂ are calculated as described in Spracklen et al. (2005a).

Oceanic DMS emissions are calculated using the ocean surface DMS concentration database of Kettle and Andreae (2000) and the sea-to-air transfer velocity according to

- 5 Nightingale et al. (2000). Emissions of biogenic terpenes are from the GEIA inventory (Benkovitz et al., 1996) and are based on Guenther et al. (1995). Emissions of SO₂ and carbonaceous aerosol from wildfires, biofuel, fossil fuel and volcanoes are based on the AEROCOM¹ emission inventories for the year 2000 (Dentener et al., 2006).

- 10 Secondary organic aerosol (SOA) from biogenic terpenes is included assuming the reactivity of alpha-pinene including reactions with OH, O₃ and NO₃ (Spracklen et al., 2006). We assume all three reactions have a constant yield of 13% to a first-stage oxidation product that condenses with zero vapour pressure onto existing aerosol (Spracklen et al., 2006). We add SOA to the hydrophilic aerosol distribution.

2.2 Primary emissions and particle formation

- 15 We test the sensitivity of the model to the emission of primary particles and the nucleation rate through a series of experiments detailed below and in Table 1.

- 20 1. Experiment PRI includes anthropogenic and natural primary particulate emissions but no secondary particle formation. Primary sea-spray emissions are based on Gong et al. (2003). We assume that a fraction of sulfur dioxide emissions are emitted as primary sulfate either because these particles are directly emitted to the atmosphere or because they are formed through gas-to-particle conversion at spatial scales smaller than our model grid. Emissions of primary sulfate are a standard option in many aerosol models (e.g., Adams and Seinfeld, 2002; Spracklen et al., 2005a; Stier et al., 2005), however the properties of the particles are very uncertain. Primary sulfate and carbonaceous (EC/OC) particles are emitted assuming lognormal modes, which are mapped onto the model size bins. We emit primary sulfate at the rate (2.5% of SO₂

¹ Available at: <http://nansen.ipsl.jussieu.fr/AEROCOM/>

[Title Page](#)

[Abstract](#)

[Introduction](#)

[Conclusions](#)

[References](#)

[Tables](#)

[Figures](#)

◀

▶

[Back](#)

[Close](#)

[Full Screen / Esc](#)

[Printer-friendly Version](#)

[Interactive Discussion](#)



emissions) and using the size distribution suggested by AEROCOM (road transport: number median radius, $r=15\text{ nm}$, $\sigma=1.8$; shipping, industry and power-plant emissions: $r=500\text{ nm}$, $\sigma=2.0$; wildfire and biofuel: $r=40\text{ nm}$, $\sigma=1.8$; volcanic emissions: 50% at $r=15\text{ nm}$ and 50% at $r=40\text{ nm}$, $\sigma=1.8$). For EC/OC emissions we use the emission size distribution suggested by Stier et al. (2005) (fossil fuel emissions: $r=30\text{ nm}$, $\sigma=1.59$, wildfire and biofuel emissions: $r=75\text{ nm}$ and $\sigma=1.59$).

2. Experiment BHN includes identical primary emissions to PRI, but additionally it includes particle formation assuming binary homogeneous $\text{H}_2\text{SO}_4\text{-H}_2\text{O}$ nucleation using the parameterization of Kulmala et al. (1998a).

10 3. Experiments PRICAR and PRISUL test the sensitivity of the model to uncertainty in the assumed size distribution of the primary emissions. Experiment PRICAR uses the AEROCOM size distribution for emissions of EC/OC particles (Dentener et al., 2006), emitting EC/OC particles at about half the diameter of experiment PRI (fossil fuel: $r=15\text{ nm}$, $\sigma=1.8$, biofuel and wildfire: $r=40\text{ nm}$, $\sigma=1.8$) and thereby increasing the emitted EC/OC number by about a factor 8. Experiment PRISUL assumes that anthropogenic primary sulfate particles (transport, shipping, industry and power-plant emissions) are emitted at the size distribution according to Adams and Seinfeld (2003) (15% of emitted mass at $r=5\text{ nm}$, $\sigma=1.6$, 85% at $r=35\text{ nm}$, $\sigma=2.0$).

15 4. Experiments ACT and KIN are as experiment BHN, but additionally they include an empirical particle formation mechanism (Kulmala et al., 2006; Sihto et al., 2006) in the BL. This mechanism is based on analysis of surface particle formation events. The formation rate (J_1) of 1-nm particles is given by:

$$J_1 = A[\text{H}_2\text{SO}_4]^M \quad (1)$$

20 where A is the nucleation coefficient. The value of M has been found to vary between 1 and 2 and A varies spatially and temporally, for reasons which are not known. We perform model simulations for both $M=1$ (activation mechanism, ACT) and $M=2$ (kinetic mechanism, KIN) and with a range of nucleation coefficients. In each model experiment the magnitude of the nucleation coefficient is fixed globally.

Explaining global aerosol number concentrations

D. V. Spracklen et al.

[Title Page](#)

[Abstract](#)

[Introduction](#)

[Conclusions](#)

[References](#)

[Tables](#)

[Figures](#)

◀

▶

◀

▶

[Back](#)

[Close](#)

[Full Screen / Esc](#)

[Printer-friendly Version](#)

[Interactive Discussion](#)



The particle formation rate at 3 nm (J_3) is obtained from J_1 and the equation of Kerminen and Kulmala (2002):

$$J_3 = J_1 \exp \left(-0.153 \frac{CS'}{GR} \right), \quad (2)$$

where CS' is the reduced condensation sink (m^{-2}) and GR (nm h^{-1}) is the cluster growth rate. GR is assumed to be constant between 1 nm and 3 nm and is calculated from the gas-phase sulfuric acid concentration. Newly formed particles are added to the model at 3 nm diameter. A full description of this mechanism in the GLOMAP model is described in Spracklen et al. (2006).

The empirical particle formation mechanism is based on observation of particle formation events made at the surface and there is some evidence to suggest that formation events are less likely in the lower FT (Heintzenberg et al., 2008; O'Dowd et al., 2009). Observations of the vertical profile of CN number concentrations typically show maxima at the surface and in the UT and a minimum in the lower FT (Clarke and Kapturin, 2002; Schröder et al., 2002; Singh et al., 2002). Applying the empirical particle formation mechanism throughout the depth of the troposphere in our model does not capture this observed profile and results in overprediction of CN concentrations in the lower FT. For this reason, as in earlier work (Spracklen et al., 2006, 2008), we restrict the empirical particle formation mechanism to the BL while allowing BHN to occur above (which results in particle formation in the UT).

20 3 Simulation of surface CN number concentrations

Simulated surface CN (diameter >3 nm) concentrations for the different experiments described in Sect. 2.2 are shown in Table 1 and Fig. 1. With no particle formation (PRI), surface annual mean (median) CN concentrations are 105 (30) cm^{-3} over the oceans and 640 (107) cm^{-3} over the continents. Greater simulated concentrations over the continents are due to primary anthropogenic emissions. BHN increases surface mean

Explaining global aerosol number concentrations

D. V. Spracklen et al.

[Title Page](#)

[Abstract](#)

[Introduction](#)

[Conclusions](#)

[References](#)

[Tables](#)

[Figures](#)

◀

▶

[Back](#)

[Close](#)

[Full Screen / Esc](#)

[Printer-friendly Version](#)

[Interactive Discussion](#)



(median) CN concentrations by a factor 3.3 (8.4) over the oceans and factor 1.5 (5.7) over the continents. The absolute increase in mean CN at the surface due to BHN is relatively uniform across the globe (average of 250 cm^{-3} over oceans and 310 cm^{-3} over continental regions). This is because the secondary source of particles from BHN is largely in the upper troposphere (UT) and somewhat independent of SO_2 sources at the surface (Raes et al., 2000). Increasing the number emission of primary EC/OC particles (PRICAR) further increases (over experiment BHN) mean (median) surface CN concentrations by a factor 1.4 (1.1) over the oceans and a factor 2.3 (1.4) over the continents. Increasing the number emissions of primary sulfate particles (PRISUL) increases CN concentrations by a factor 1.7 (1.1) over the oceans and a factor 2.4 (1.2) over the continents. The empirical BL particle formation scheme (with $M=1$ and $k=2\times10^{-6}\text{ s}^{-1}$) increases mean (median) surface CN concentrations by a factor of 2.1 (1.9) over the oceans and by a factor of 1.8 (1.4) over the continents. Surface CN concentrations are sensitive to the nucleation coefficient used: a factor 100 change in the BL nucleation coefficient (A in Eq. 1) changes J_1 by a factor 100 and increases the surface CN concentration by a factor of 2.3. In contrast, surface CN are relatively insensitive to changes in the BHN nucleation rate, changing by less than 40% for factor 100 change in the BHN rate (Spracklen et al., 2005b). This is because BHN occurs primarily in the UT and coagulation that occurs during transport and mixing of air to the surface reduces the sensitivity of surface CN to changes in BHN rate. The sensitivity of surface CN concentrations to the BL particle formation rate allows us to use observed CN concentrations and a global model to give a constraint to the global nucleation rate as we show below (Sect. 4.2).

Explaining global aerosol number concentrations

D. V. Spracklen et al.

[Title Page](#)

[Abstract](#)

[Introduction](#)

[Conclusions](#)

[References](#)

[Tables](#)

[Figures](#)

◀

▶

◀

▶

[Back](#)

[Close](#)

[Full Screen / Esc](#)

[Printer-friendly Version](#)

[Interactive Discussion](#)



4 Model evaluation

4.1 The CN dataset

To evaluate the model we compiled a dataset of surface CN number concentrations recorded at 36 sites around the world. The locations of the sites are shown in Fig. 2 and Table 2. We broadly classified the sites into FT, MBL and continental BL. We did not include any sites within urban environments because the resolution of our model is not sufficient to resolve urban-scale pollution. We only included sites which have recorded CN concentrations for at least a 12 month period. At sites with more than 12 months of data we report monthly mean and median concentrations as an average over the multiannual dataset. The time period of observations used at each site is shown in Table 2. To give an indication of the interannual variability in the observations we report the standard deviation in monthly mean CN concentrations at sites where there are 4 or more years of data available.

Observations of CN were made either using condensation particle counters (CPCs), scanning mobility particle sizers (SMPS) or differential mobility particle sizers (DMPS). CPCs record total particle number concentration typically for sizes greater than 3 nm or 10 nm in diameter. SMPS and DMPS record the particle size distribution at sizes greater than either 3 nm or 10 nm in diameter. From the observed size distribution a CN concentration was calculated. We compared model experiments for each site using the same lower cutoff diameter as available from the observations. All CN concentrations are reported at ambient temperature and pressure.

All the MBL sites in this analysis are at coastal locations which are influenced by continental emissions (except Samoa which is at a very remote site in the tropical Pacific and probably experiences minimal continental influence). We did not screen the data in an attempt to remove continental influence (e.g., Reade et al., 2006) as this complicates analysis with a 3-D Eulerian model.

High altitude sites located near the top of mountains are often influenced by thermal winds resulting in diurnal cycles in aerosol (Venzac et al., 2009). Additionally, diurnal

Explaining global aerosol number concentrations

D. V. Spracklen et al.

[Title Page](#)

[Abstract](#)

[Introduction](#)

[Conclusions](#)

[References](#)

[Tables](#)

[Figures](#)

◀

▶

◀

▶

[Back](#)

[Close](#)

[Full Screen / Esc](#)

[Printer-friendly Version](#)

[Interactive Discussion](#)



and seasonal variation of BL height means mountain sites can be located in either the BL or FT at different times of the day or year. For these reasons the data from high altitude sites may not represent background FT conditions without detailed screening which was not performed here. Nevertheless, the model does simulate variations in
5 BL height though they have not been evaluated specifically at the locations analysed in this study.

We linearly interpolate the model to the horizontal location of the observations. Where sub-grid topography means that the altitude above sea-level of the observation site is not within 500 m of the grid-point elevation of the model surface level (TOMCAT
10 uses hybrid σ -pressure coordinates), we interpolate the model in the vertical to match the altitude of the observations.

4.2 Global analysis of annual mean CN number concentrations

Figure 3 compares simulated and observed annual mean CN number concentrations. Observed annual mean CN concentrations at MBL and FT sites are less than
15 2000 cm⁻³. The lowest concentrations are observed at the South Pole in Antarctica (100 cm⁻³), Samoa in the tropical MBL (300 cm⁻³), coastal Antarctica (350 cm⁻³) and Point Barrow in the Arctic (450 cm⁻³). The mid-latitude MBL sites in this analysis are at coastal locations influenced by continental aerosol sources and have CN concentrations of between 950 cm⁻³ and 1750 cm⁻³. We did not filter out such a continental
20 influence and so the MBL concentrations we report may not be representative for the open ocean. Observed CN concentrations at continental BL sites are up to an order of magnitude greater, spanning 800 cm⁻³ to 7000 cm⁻³.

Figure 3 also shows the equation of the linear regression fits between model and observations. Model bias between is further quantified as a normalised mean bias
25 (NMB=100× $\sum_{i=1}^n(S_i-O_i)/\sum_{i=1}^nO_i$, where S_i is the simulated annual mean CN concentration and O_i is the observed annual mean CN concentration at site i) shown in Table 3.

Explaining global aerosol number concentrations

D. V. Spracklen et al.

[Title Page](#)

[Abstract](#)

[Introduction](#)

[Conclusions](#)

[References](#)

[Tables](#)

[Figures](#)

◀

▶

◀

▶

[Back](#)

[Close](#)

[Full Screen / Esc](#)

[Printer-friendly Version](#)

[Interactive Discussion](#)



The experiment with natural and anthropogenic primary particulate emissions but no secondary particle formation (PRI) captures the spatial pattern of CN concentrations relatively well ($R^2=0.51$) but underestimates concentrations at all sites (slope of the linear regression, $m=0.29$, NMB=−77%). Simulated concentrations at continental BL sites are underpredicted by a factor of 2–10, and FT and MBL sites are underpredicted by up to a factor of 10 or more.

Including binary homogeneous nucleation in the model (BHN) increases simulated BL CN concentrations by 200–400 cm^{−3} and FT CN by up to 1000 cm^{−3} but results in only a modest reduction in model bias across all sites ($m=0.32$, NMB=−61%). Simulated concentrations are most improved at FT sites (NMB=−25%) and annual mean particle number at FT sites are mostly predicted within a factor of 2. CN concentrations at MBL sites are still underpredicted (NMB=−61%). However, annual mean CN concentrations are well simulated at Samoa which is the only remote MBL site in this analysis.

Increasing the number emission of primary anthropogenic particulate emissions (by reducing the assumed diameter of the emissions) increases simulated BL CN concentrations by as much as 10 000 cm^{−3}. The impact in the BL is regionally dependent: at sites close to anthropogenic sources (e.g., Finokalia, Hohenpeissenberg, Bondville, South Great Plains) simulated CN increases by up to a factor of 2.5, whereas at remote BL sites (e.g., South Pole, Point Barrow, Samoa, Cape Grim) they increase by less than 30%. Increasing EC/OC number emission (PRICAR) results in a smaller model bias ($m=0.93$, NMB=−12%) whereas increasing primary sulfate (PRISUL) results in model overprediction ($m=1.47$, NMB=34%). Such a large increase in simulated CN concentrations due to primary emissions has been seen in previous work such as Pierce and Adams (2009).

Including BL particle formation increases annual mean CN concentrations at BL sites by several thousand cm^{−3}, similar to that simulated by increasing anthropogenic primary emissions. With the activation (ACT) particle formation mechanism, model bias varies from −44% to 17% with the best match between model and observations

Explaining global aerosol number concentrations

D. V. Spracklen et al.

[Title Page](#)

[Abstract](#)

[Introduction](#)

[Conclusions](#)

[References](#)

[Tables](#)

[Figures](#)

◀

▶

◀

▶

[Back](#)

[Close](#)

[Full Screen / Esc](#)

[Printer-friendly Version](#)

[Interactive Discussion](#)



occurring using a nucleation coefficient of between $A=2\times10^{-6}$ and $A=2\times10^{-5}\text{ s}^{-1}$. With the kinetic (KIN) particle formation mechanism, model bias varies between -35% and 31% with the best match occurring when $A=2\times10^{-12}\text{ cm}^3\text{ s}^{-1}$. These derived nucleation rate coefficients lie within the range of values calculated from observed particle formation rates: activation mechanism $A=3.3\times10^{-8}\text{ s}^{-1}$ – $3.5\times10^{-4}\text{ s}^{-1}$ (Riipinen et al., 2007); kinetic mechanism $A=2.4\times10^{-15}\text{ cm}^3\text{ s}^{-1}$ – $1.3\times10^{-10}\text{ cm}^3\text{ s}^{-1}$ (Riipinen et al., 2007; Kuang et al., 2008).

Our analysis provide support for previous work (Riipinen et al., 2007; Kuang et al., 2008) that the magnitude of the BL nucleation rate coefficient varies spatially. Observed CN concentrations at Arctic and boreal forest sites (Pallas and Hyytiälä) are well matched by the model with $A=2\times10^{-6}\text{ s}^{-1}$ ($M=1$) or $2\times10^{-13}\text{ cm}^3\text{ s}^{-1}$ ($M=2$). Sites in the Midwest US (Bondville and South Great Plains) would require a nucleation coefficient greater than $A=2\times10^{-5}\text{ s}^{-1}$ ($M=1$) to match observed CN. The reason for variability in the nucleation rate coefficient is unknown, but could include varying concentrations of other atmospheric species that can stabilise sulfate clusters. It has been suggested that organic species may be a key candidate (Verheggen et al., 2007; Bonn et al., 2008). The model underpredicts CN concentrations at mid-latitude MBL sites even with the largest nucleation coefficient used in this analysis. This may be due to alternative nucleation mechanisms being important in these locations (O'Dowd et al., 2002).

The spatial pattern of annual mean CN concentrations can be best captured by either increasing the number emission of primary anthropogenic emissions, PRICAR ($R^2=0.57$) and PRISUL ($R^2=0.60$), or through including BL particle formation, ACT2 ($R^2=0.58$) and KIN2 ($R^2=0.57$). Previous studies, using a smaller dataset than we compiled here, have also shown that it is difficult to constrain particle formation and primary emissions using annual mean particle number concentrations. To provide a stronger constraint on primary emissions and particle formation we therefore examined the observed seasonal cycle of particle number.

Explaining global aerosol number concentrations

D. V. Spracklen et al.

[Title Page](#)

[Abstract](#)

[Introduction](#)

[Conclusions](#)

[References](#)

[Tables](#)

[Figures](#)

◀

▶

◀

▶

[Back](#)

[Close](#)

[Full Screen / Esc](#)

[Printer-friendly Version](#)

[Interactive Discussion](#)



4.3 Accounting for the seasonal cycle in CN

ACPD

9, 26377–26419, 2009

Figures 4, 5 and 6 show the seasonal cycle of observed and simulated CN concentrations at FT, MBL and continental BL sites. At many locations a pronounced seasonal cycle is observed, with summer-time CN concentrations exceeding winter-time concentrations by a factor of 2–10. For example, at the South Pole summertime CN concentrations are about 250 cm^{-3} whereas wintertime concentrations are less than 20 cm^{-3} . In Pallas, Finland, summertime CN concentrations are about 1250 cm^{-3} whereas wintertime concentrations are about 250 cm^{-3} .

Table 4 shows the correlation coefficient between simulated and observed monthly mean CN concentrations for sites where monthly mean CN concentrations vary by more than a factor of 2 throughout the seasonal cycle. Figure 7 shows the average correlation coefficients for these sites calculated separately for FT, MBL and continental BL sites.

The model experiment with only primary particulate emissions (PRI) does not capture the observed seasonal cycle demonstrated by the poor correlation coefficient between simulated and observed monthly mean CN concentrations at FT ($R^2=0.09$), MBL ($R^2=0.14$) and continental BL sites ($R^2=0.11$). With BHN the model captures the observed seasonal cycle at some MBL (e.g., Neumayer) and FT sites (e.g., South Pole, Mt. Washington) resulting in a better correlation in both the FT ($R^2=0.26$) and MBL ($R^2=0.36$). While winter-time concentrations are relatively well simulated at some BL sites (e.g., Point Barrow, Hyttälä and Pallas) underprediction during summer months results in a poorly represented seasonal cycle in the continental BL ($R^2=0.1$). Increasing primary emissions degrades model representation of the seasonal cycle in the FT (PRICAR, $R^2=0.12$, PRISUL, $R^2=0.22$) and MBL (PRICAR, $R^2=0.21$, PRISUL, $R^2=0.36$), while slightly improving simulation in the continental BL (PRICAR, $R^2=0.14$, PRISUL, $R^2=0.18$). Including BLN particle formation improves the simulated seasonal cycle at continental BL sites (ACT2, $R^2=0.25$; KIN2 $R^2=0.30$) whilst maintaining

Explaining global aerosol number concentrations

D. V. Spracklen et al.

[Title Page](#)

[Abstract](#)

[Introduction](#)

[Conclusions](#)

[References](#)

[Tables](#)

[Figures](#)

◀

▶

◀

▶

[Back](#)

[Close](#)

[Full Screen / Esc](#)

[Printer-friendly Version](#)

[Interactive Discussion](#)



or improving representation of the seasonal cycle in the FT (ACT2, $R^2=0.27$; KIN2 $R^2=0.36$) and MBL (ACT2, $R^2=0.34$; KIN2 $R^2=0.43$).

4.4 Additional remote marine CN measurements

To extend the evaluation of the model to the remote MBL we use the dataset of
5 Heintzenberg et al. (2000) who compiled observations from several field campaigns
including ACE-1, ACE-2, ACE-Asia and INDOEX. Heintzenberg et al. (2000) fitted ob-
served aerosol size distributions with two lognormal modes and gridded the observa-
tions into 15° latitude bands. The different field campaigns used a range of sampling
instruments with lower cutoff diameters ranging from 3 nm to 12 nm, but this information
10 was not captured by the analysis.

Figure 8 shows CN concentrations from the Heintzenberg et al. (2000) dataset com-
pared with our model. We plot simulated CN (diameter >12 nm), which over the oceans
is virtually identical to simulated CN (diameter >3 nm), except when BL particle forma-
tion is included in the model. For this experiment we plot both CN (diameter >3 nm)
15 and CN (diameter >12 nm).

With primary emissions only (PRI) the model underestimates CN concentrations at
all latitudes except 30°–45° N. When binary homogeneous nucleation is included (BHN)
the model still underpredicts CN concentrations in the Southern Hemisphere (between
15° S and 75° S) and Arctic (between 75° N and 90° N) oceans while either well simulat-
20 ing or overpredicting CN elsewhere in the Northern Hemisphere. Such underprediction
in the Southern Hemisphere is a consistent feature of global aerosol models (Easter
et al., 2004; Spracklen et al., 2005a,b; Pierce and Adams, 2006; Pierce et al., 2007;
Trivitayanurak et al., 2008; Wang et al., 2009). Underprediction of CN above 75° N is
likely due to the model not well simulating the transport of anthropogenic pollution to
25 the Arctic (Korhonen et al., 2008). Increasing the number emission from primary an-
thropogenic sources results in overprediction of CN between 15° N and 60° N, while
the underprediction of CN persists in the Southern Hemisphere and Arctic. Including

Explaining global aerosol number concentrations

D. V. Spracklen et al.

[Title Page](#)

[Abstract](#)

[Introduction](#)

[Conclusions](#)

[References](#)

[Tables](#)

[Figures](#)

◀

▶

◀

▶

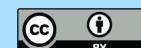
[Back](#)

[Close](#)

[Full Screen / Esc](#)

[Printer-friendly Version](#)

[Interactive Discussion](#)



BL particle formation increases simulated CN, particularly in regions of SO_2 emissions from shipping and DMS emissions from the ocean. In the Southern Hemisphere, BL particle formation scheme improves the simulation of CN, whereas in the Northern Hemisphere it results in overprediction of CN except in the Arctic where the model underprediction of CN remains. Emissions of ultrafine sea-spray (Mårtensson et al., 2003), not included in this work, may be another explanation for underprediction of CN in the Southern Ocean (Pierce and Adams, 2006).

5 Summary and conclusions

We have used the GLOMAP global aerosol microphysics model to simulate global CN number concentrations and evaluated the model against observations compiled from 36 surface sites around the globe. Our aim was to evaluate the role of primary particulate emissions and particle formation in controlling regional and global surface CN concentrations.

We conducted a range of experiments with different assumptions about primary anthropogenic emissions and particle formation. Without secondary particle formation (primary particulate emissions only) the model greatly underpredicts observed CN concentrations ($\text{NMB}=-77\%$). While the spatial pattern of observed CN is relatively well captured ($R^2=0.51$) the model does not capture the seasonal cycle observed at FT ($R^2=0.09$), MBL ($R^2=0.14$) or continental BL sites ($R^2=0.11$).

Including binary homogeneous nucleation of $\text{H}_2\text{SO}_4\text{-H}_2\text{O}$ (Kulmala et al., 1998a) in addition to primary emissions reduces model bias at FT sites ($\text{NMB}=-25\%$) and improves the simulated seasonal cycle in the MBL ($R^2=0.36$) and FT ($R^2=0.26$). However, CN is still underpredicted in the continental BL resulting in little improvement in model bias ($\text{NMB}=-66\%$) or representation of the seasonal cycle ($R^2=0.1$) at these sites.

There is considerable uncertainty in the size distribution of primary anthropogenic particulate emissions (which affects the particle number emitted for fixed mass) and

Explaining global aerosol number concentrations

D. V. Spracklen et al.

[Title Page](#)

[Abstract](#)

[Introduction](#)

[Conclusions](#)

[References](#)

[Tables](#)

[Figures](#)

◀

▶

[Back](#)

[Close](#)

[Full Screen / Esc](#)

[Printer-friendly Version](#)

[Interactive Discussion](#)



previous studies have used a range of assumptions. We therefore evaluated the sensitivity of simulated CN to the uncertainty in the anthropogenic primary sulfate and carbonaceous aerosol size distributions. Reducing the emissions size of primary carbonaceous (PRICAR) or sulfate (PRISUL) particles (and so increasing the number emission) within the range assumed by previous studies slightly improves the spatial pattern of simulated CN (PRICAR, $R^2=0.57$; PRISUL, $R^2=0.6$) and reduces the model bias (PRICAR, NMB=-12%; PRISUL, NMB=34%) (these experiments included particle formation through binary homogeneous nucleation). However, scaling the anthropogenic primary emissions in this way does not improve the simulated seasonal cycle, slightly degrading model performance in the MBL (PRICAR, $R^2=0.21$; PRISUL, $R^2=0.36$) and FT (PRICAR, $R^2=0.12$; PRISUL, $R^2=0.22$) while only slightly improving the model in the continental BL (PRICAR, $R^2=0.14$; PRISUL, $R^2=0.18$).

We tested an empirical nucleation mechanism which assumes that the formation rate of 1-nm nuclei is proportional to sulfuric acid concentration to the power 1 (activation mechanism) or 2 (kinetic mechanism). We limited the empirical mechanism to the BL and allowed binary homogeneous nucleation to occur above. When the model included a combination of these mechanisms along with primary emissions the model captured both the spatial pattern of annual mean CN (activation, $R^2=0.58$; kinetic, $R^2=0.57$) and the seasonal cycle of CN in the FT (activation, $R^2=0.27$; kinetic, $R^2=0.36$), MBL (activation, $R^2=0.34$; kinetic, $R^2=0.43$) and continental BL (activation, $R^2=0.25$; kinetic, $R^2=0.30$).

The simulated nucleation rate depends on the nucleation rate coefficient, A , the magnitude of which is poorly known. We constrained this coefficient by running multiple experiments with different rates and finding the experiment that most reduced the model bias. The best agreement was with $A=2\times10^{-6}\text{ s}^{-1}$ to $A=2\times10^{-5}\text{ s}^{-1}$ for the activation scheme and with $A=2\times10^{-12}\text{ cm}^{-3}\text{ s}^{-1}$ for the kinetic scheme, which agree with the rates derived from observed particle formation events (Riipinen et al., 2007; Kuang et al., 2008).

Explaining global aerosol number concentrations

D. V. Spracklen et al.

[Title Page](#)

[Abstract](#)

[Introduction](#)

[Conclusions](#)

[References](#)

[Tables](#)

[Figures](#)

◀

▶

◀

▶

[Back](#)

[Close](#)

[Full Screen / Esc](#)

[Printer-friendly Version](#)

[Interactive Discussion](#)



The applicability of the BL particle formation mechanism over oceanic regions requires further analysis. Observed CN concentrations at a remote tropical MBL site (Samoa) is well matched by the model with binary homogeneous nucleation. All the other MBL sites used in this analysis are at coastal locations influenced by continental emissions and therefore may not well represent remote MBL conditions unless a detailed screening of the observations is performed. The model underpredicts CN at some coastal locations (e.g., Mace Head) even with the fastest BL nucleation rates used in this study. This may be due to alternate nucleation mechanisms driven by iodine compounds being important in these locations (O'Dowd et al., 2002; Vuollekoski et al., 2009).

Long-term datasets of the seasonal variability in CN are not available for open ocean regions away from continental influence. In place of such observations we used a compilation of data from several field campaigns that has been gridded into 15° oceanic latitude bands (Heintzenberg et al., 2000). Without particle formation the model greatly underpredicts CN throughout the global oceans. As seen in previous studies, models that include primary emissions and binary homogeneous nucleation consistently underpredict CN concentrations in the Southern Ocean whilst either well predicting or overpredicting CN in the Northern Hemisphere. Over the Northern Hemisphere oceans, BL nucleation results in further overprediction of CN, whereas over the Southern Ocean BL particle formation improves simulated CN concentrations.

We have shown that particle formation is important for global aerosol concentrations. In Merikanto et al. (2009) we use the BL particle formation rate constrained in this study to quantify the contribution of primary particles and particle formation to global CN and CCN.

Explaining global aerosol number concentrations

D. V. Spracklen et al.

[Title Page](#)

[Abstract](#)

[Introduction](#)

[Conclusions](#)

[References](#)

[Tables](#)

[Figures](#)

◀

▶

◀

▶

[Back](#)

[Close](#)

[Full Screen / Esc](#)

[Printer-friendly Version](#)

[Interactive Discussion](#)



Acknowledgements. This work was supported through NERC APPRAISE, NERC AERO-FORM NE/D01395X/1 and EUCAARI. We acknowledge the UK Air Quality Archive (<http://www.airquality.co.uk/>), EU CREATE (<http://tarantula.nilu.no/projects/ccc/create/>), EU EU-SAAR (<http://ebas.nilu.no>), Global Atmospheric Watch World Data Centre for Aerosols (<http://wdca.jrc.ec.europa.eu/>), Atmospheric Investigation, Regional, Modeling, Analysis and Prediction (AIRMAP) program (www.airmap.unh.edu), British Atmospheric Data Centre (<http://badc.nerc.ac.uk/home/>), US Department of Energy, Atmospheric Radiation Measurements program (ARM) for provision of data.

References

- 10 Aalto, P., Hämeri, K., Becker, E., Weber, R., Salm, J., Mäkelä, J., Hoell, C., O'Dowd, C., Karlsson, H., Hansson, H.-C., Väkevä, M., Koponen, I., Buzorius, G., and Kulmala, M.: Physical characterization of aerosol particles during nucleation events, *Tellus B*, 53, 344–358, 2001. 26409
- 15 Adams, P. and Seinfeld, J.: Predicting global aerosol size distributions in general circulation models, *J. Geophys. Res.*, 107(D19), 4370, doi:10.1029/2001JD001010, 2002. 26381, 26382, 26384
- Adams, P. and Seinfeld, J.: Disproportionate impact of particulate emissions on global cloud condensation nuclei concentrations, *Geophys. Res. Lett.*, 30(5), 43–46, 2003. 26381, 26382, 26385, 26408
- 20 Anttila, T., Vehkamäki, H., Napari, I., and Kulmala, M.: Effect of ammonium bisulfate formation on atmospheric water-sulphuric acid-ammonia nucleation, *Boreal Environ. Res.*, 10, 511–523, 2005. 26381
- Arnold, S., Chipperfield, M., and Blitz, M.: A three-dimensional model study of the effect of new temperature-dependent quantum yields for acetone photolysis, *J. Geophys. Res.*, 110, D22305, doi:10.1029/2005JD005998, 2005. 26384
- 25 Benkovitz, C., Scholtz, M., Pacyna, J., Tarrasón, L., Dignon, J., Voldner, E., Spiro, P., Logan, J., and Graedel, T.: Global gridded inventories of anthropogenic emissions of sulfur and nitrogen, *J. Geophys. Res.*, 101(D22), 29239–29253, 1996. 26384
- Birmili, W. and Wiedensohler, A.: New particle formation in the continental boundary layer:

Explaining global aerosol number concentrations

D. V. Spracklen et al.

[Title Page](#)

[Abstract](#)

[Introduction](#)

[Conclusions](#)

[References](#)

[Tables](#)

[Figures](#)

◀

▶

[Back](#)

[Close](#)

[Full Screen / Esc](#)

[Printer-friendly Version](#)

[Interactive Discussion](#)



Meteorological and gas phase parameter influence, *Geophys. Res. Lett.*, 27(20), 3325–3328, 2000. 26380

Birmili, W., Berresheim, H., Plass-Dülmer, C., Elste, T., Gilge, S., Wiedensohler, A., and Uhrner, U.: The Hohenpeissenberg aerosol formation experiment (HAFEX): a long-term study including size-resolved aerosol, H_2SO_4 , OH, and monoterpenes measurements, *Atmos. Chem. Phys.*, 3, 361–376, 2003,
<http://www.atmos-chem-phys.net/3/361/2003/>. 26409

Bodhaine, B.: Aerosol measurements at four background sites, *J. Geophys. Res.*, 88, 10753–10768, 1983. 26409

Bonn, B., Kulmala, M., Riipinen, I., Sihto, S.-L., and Ruuskanen, T.: How biogenic terpenes govern the correlation between sulfuric acid concentrations and new particle formation, *J. Geophys. Res.*, 113, D12209, doi:10.1029/2007JD009327, 2008. 26391

Boy, M., Kazil, J., Lovejoy, E., Guenther, A., and Kulmala, M.: Relevance of ion-induced nucleation of sulfuric acid and water in the lower troposphere over the boreal forest at northern latitudes, *Atmos. Res.*, 90, 151–158, 2008. 26381

Chang, L.-S., Schwartz, S., McGraw, R., and Lewis, E.: Sensitivity of aerosol properties to new particle formation mechanism and to primary emissions in a continental-scale chemical transport model, *J. Geophys. Res.*, 114, D07203, doi:10.1029/2008JD011019, 2009. 26382

Charron, A., Birmili, W., and Harrison, R.: Factors influencing new particle formation at the rural site, Harwell, UK, *J. Geophys. Res.*, 112, D14210, doi:10.1029/2007JD008425, 2007. 26409

Chipperfield, M.: New version of the TOMCAT/SLIMCAT off-line chemical transport model: intercomparison of stratospheric tracer experiments, *Q. J. Roy. Meteorol. Soc.*, 132, 1179–1203, doi:10.1256/qj.05.51, 2006. 26383

Clarke, A. and Kapustin, V.: A pacific aerosol survey. Part I: A decade of data on particle production, transport, evolution, and mixing in the troposphere, *J. Atmos. Sci.*, 59(3), 363–382, 2002. 26386

Clarke, A., Davis, D., Kapustin, V., Eisele, F., Chen, G., Paluch, I., Lenschow, D., Bandy, A., Thornton, D., Moore, K., Mauldin, L., Tanner, D., Litchy, M., Carroll, M., Collins, J., and Albercook, G.: Particle nucleation in the tropical boundary layer and its coupling to marine sulfur sources, *Science*, 282, 89–92, 1998. 26380

Clarke, A., Eisele, F., Kapustin, V., Moore, K., Tanner, D., Mauldin, L., Litchy, M., Lienert, B., Carroll, M., and Albercook, G.: Nucleation in the equatorial free troposphere: Favorable environments during PEM-Tropics, *J. Geophys. Res.*, 104(D5), 5735–5744, 1999. 26380

Explaining global aerosol number concentrations

D. V. Spracklen et al.

[Title Page](#)

[Abstract](#)

[Introduction](#)

[Conclusions](#)

[References](#)

[Tables](#)

[Figures](#)

◀

▶

◀

▶

[Back](#)

[Close](#)

[Full Screen / Esc](#)

[Printer-friendly Version](#)

[Interactive Discussion](#)



- Dal Maso, M., Kulmala, M., Riipinen, I., Wagner, R., Hussein, T., Aalto, P., and Lehtinen, K.: Formation and growth of fresh atmospheric aerosols: eight years of aerosol size distribution data from SMEAR II, Hyttiälä, Finland, *Boreal Environ. Res.*, 10, 323–336, 2005. 26380
- Dal Maso, M., Hyvärinen, A., Komppula, M., Tunved, P., Kerminen, V.-M., Lihavainen, H., Viisanen, Y., Hansson, H.-C., and Kulmala, M.: Annual and interannual variation in boreal forest aerosol particle number and volume concentration and their connection to particle formation, *Tellus*, 60B, 495–508, 2008a. 26409
- Dal Maso, M., Sogacheva, L., Anisimov, M., Arshinov, M., Baklanov, A., Belan, B., Khodzher, T., Obolkin, V., Staroverova, A., Vlasov, A., Zagaynov, V., Lushnikov, A., Lyubovtseva, Y., Riipinen, I., Kerminen, V.-M., and Kulmala, M.: Aerosol particle formation events at two Siberian stations inside the boreal forest, *Boreal Environ. Res.*, 13, 81–92, 2008b. 26409
- Delene, D. and Ogren, J.: Variability of aerosol optical properties at four North American surface monitoring sites, *J. Atmos. Sci.*, 59, 1135–1150, 2002. 26409
- Dentener, F., Kinne, S., Bond, T., Boucher, O., Cofala, J., Generoso, S., Ginoux, P., Gong, S., Hoelzemann, J. J., Ito, A., Marelli, L., Penner, J. E., Putaud, J.-P., Textor, C., Schulz, M., van der Werf, G. R., and Wilson, J.: Emissions of primary aerosol and precursor gases in the years 2000 and 1750 prescribed data-sets for AeroCom, *Atmos. Chem. Phys.*, 6, 4321–4344, 2006,
<http://www.atmos-chem-phys.net/6/4321/2006/>. 26384, 26385
- Easter, R., Ghan, S., Zhang, Y., Saylor, R., Chapman, E., Laulainen, N., Abdul-Razzak, H., Leung, L., Bian, X., and Zaveri, R.: MIRAGE: Model description and evaluation of aerosols and trace gases, *J. Geophys. Res.*, 109, D20210, doi:10.1029/2004JD004571, 2004. 26381, 26382, 26393
- Elleman, R. A. and Covert, D.: Aerosol size distribution modeling with the community multiscale air quality modeling system in the Pacific Northwest: 2. parameterizations for ternary nucleation and nucleation mode processes, *J. Geophys. Res.*, 114, D11207, doi:10.1029/2009JD012187, 2009. 26381
- Gaydos, T. M., Stanier, C., and Pandis, S.: Modeling of in situ ultrafine atmospheric particle formation in the eastern United States, *J. Geophys. Res.*, 110, D07S12, doi:10.1029/2004JD004683, 2005. 26380
- Gong, S., Barrie, L., Blanchet, J.-P., von Salzen, K., Lohmann, U., Lesins, G., Spacek, L., Zhang, L., Girard, E., Lin, H., Leaitch, R., Leighton, H., Chylek, P., and Huang, P.: Canadian aerosol module: A size-segregated simulation of atmospheric aerosol processes for

Explaining global aerosol number concentrations

D. V. Spracklen et al.

[Title Page](#)

[Abstract](#)

[Introduction](#)

[Conclusions](#)

[References](#)

[Tables](#)

[Figures](#)

◀

▶

◀

▶

[Back](#)

[Close](#)

[Full Screen / Esc](#)

[Printer-friendly Version](#)

[Interactive Discussion](#)



- climate and air quality models 1. Module development, *J. Geophys. Res.*, 108, 4007, doi:10.1029/2001JD002002, 2003. 26384
- Gras, J.: CN, CCN and particle size in Southern Ocean air at Cape Grim, *Atmos. Res.*, 35, 233–251, 1995. 26409
- 5 Guenther, A., Hewitt, C., Erickson, D., Geron, C., Graedal, T., Harley, P., Klinger, L., Lerdau, M., McKay, W., Pierce, T., Scholes, B., Steinbrecher, R., Tallamraju, R., Taylor, J., and Zimmerman, P.: A global model of natural volatile organic compound emissions, *J. Geophys. Res.*, 100(D5), 8873–8892, 1995. 26384
- 10 Hamed, A., Joutsensaari, J., Mikkonen, S., Sogacheva, L., Dal Maso, M., Kulmala, M., Cavalli, F., Fuzzi, S., Facchini, M. C., Decesari, S., Mircea, M., Lehtinen, K. E. J., and Laaksonen, A.: Nucleation and growth of new particles in Po Valley, Italy, *Atmos. Chem. Phys.*, 7, 355–376, 2007, <http://www.atmos-chem-phys.net/7/355/2007/>. 26409
- 15 Heintzenberg, J., Covert, D., and Van Dingenen, R.: Size distribution and chemical composition of marine aerosols: a compilation and review, *Tellus B*, 52, 1104–1122, 2000. 26393, 26396, 26419
- Heintzenberg, J., Birmili, W., Theiss, D., and Kisilyakhov, Y.: The atmospheric aerosol over Siberia, as seen from the 300 m ZOTTO tower, *Tellus*, 60B, 276–285, doi:10.1111/j.1600–0889.2007.00335.x, 2008. 26386
- 20 Jaeger-Voirol, A. and Mirabel, P.: Nucleation rate in a binary mixture of sulfuric acid and water vapour, *J. Phys. Chem.*, 92, 3518–3521, 1988. 26380
- Kazil, J., Lovejoy, E. R., Barth, M. C., and O'Brien, K.: Aerosol nucleation over oceans and the role of galactic cosmic rays, *Atmos. Chem. Phys.*, 6, 4905–4924, 2006, <http://www.atmos-chem-phys.net/6/4905/2006/>. 26381
- 25 Kerminen, V.-M. and Kulmala, M.: Analytical formulae connecting the “real” and the apparent nucleation rate and the nuclei number concentration for atmospheric nucleation events, *J. Aerosol Sci.*, 33, 609–622, 2002. 26386
- Kettle, A. and Andreae, M.: Flux of dimethylsulfide from the oceans: A comparison of updated data sets and flux models, *J. Geophys. Res.*, 105, 26793–26808, 2000. 26384
- 30 Kivekäs, N., Sun, J., Zhan, M., Kerminen, V.-M., Hyvärinen, A., Komppula, M., Viisanen, Y., Hong, N., Zhang, Y., Kulmala, M., Zhang, X.-C., Deli-Geer, and Lihavainen, H.: Long term particle size distribution measurements at Mount Waliguan, a high-altitude site in inland China, *Atmos. Chem. Phys.*, 9, 5461–5474, 2009,

Explaining global aerosol number concentrations

D. V. Spracklen et al.

[Title Page](#)

[Abstract](#)

[Introduction](#)

[Conclusions](#)

[References](#)

[Tables](#)

[Figures](#)

◀

▶

[Back](#)

[Close](#)

[Full Screen / Esc](#)

[Printer-friendly Version](#)

[Interactive Discussion](#)



- http://www.atmos-chem-phys.net/9/5461/2009/. 26409
Komppula, M., Lihavainen, H., Hatakka, J., Paatero, J., Aalto, P., Kulmala, M., and Viisanen, Y.: Observations of new particle formation and size distributions at two different heights and surroundings in subarctic area in northern Finland, *J. Geophys. Res.*, 108(D9), 4295, doi:10.1029/2002JD002939, 2003. 26409
- 5 Komppula, M., Sihto, S.-L., Korhonen, H., Lihavainen, H., Kerminen, V.-M., Kulmala, M., and Viisanen, Y.: New particle formation in air mass transported between two measurement sites in Northern Finland, *Atmos. Chem. Phys.*, 6, 2811–2824, 2006, http://www.atmos-chem-phys.net/6/2811/2006/. 26380
- 10 Komppula, M., Lihavainen, H., Hyvärinen, A.-P., Kerminen, V.-M., Panwar, T., Sharma, V., and Viisanen, Y.: Physical properties of aerosol particles at a Himalayan background site in India, *J. Geophys. Res.*, 114, D12202, doi:10.1029/2008JD011007, 2009. 26409
- 15 Koponen, I. K., Virkkula, A., Hillamo, R., Kerminen, V.-M., and Kulmala, M.: Number size distributions and concentrations of the continental summer aerosols in Queen Maud Land, Antarctica, *J. Geophys. Res.*, 108(D18), 4587, doi:10.1029/2003JD003614, 2003. 26380
- Korhonen, H., Carslaw, K., Spracklen, D., Ridley, D., and Ström, J.: A global model study of processes controlling aerosol size distributions in the Arctic spring and summer, *J. Geophys. Res.*, 113, D08211, doi:10.1029/2007JD009114, 2008. 26393
- 20 Kuang, C., McMurry, P., McCormick, A., and Eisele, F.: Dependence of nucleation rates on sulfuric acid vapor concentrations in diverse atmospheric locations, *J. Geophys. Res.*, 113, D10209, doi:10.1029/2007JD009253, 2008. 26381, 26391, 26395
- Kuang, C., McMurry, P., and McCormick, A.: Determination of cloud condensation nuclei production from measured new particle formation events, *Geophys. Res. Lett.*, 36, L09822, doi:10.1029/2007JD009253, 2009. 26380, 26383
- 25 Kulmala, M., Laaksonen, A., and Pirjola, L.: Parameterizations for sulfuric acid/water nucleation rates, *J. Geophys. Res.*, 103(D7), 8301–8307, 1998a. 26380, 26385, 26394
- Kulmala, M., Toivonen, A., Mäkelä, J., and Laaksonen, A.: Analysis of the growth of nucleation mode particles observed in boreal forest, *Tellus B*, 50B, 449–462, 1998b. 26380
- 30 Kulmala, M., Dal Maso, M., Mäkelä, J., Pirjola, L., Väkevä, M., Aalto, P., Miikkulainen, P., Hämeri, K., and O'Dowd, C.: On the formation, growth and composition of nucleation mode particles, *Tellus B*, 53B, 479–490, 2001. 26380
- Kulmala, M., Vehkamäki, H., Petajda, T., Dal Maso, M., Lauri, A., Kerminen, V., Birmili, W., and McMurry, P.: Formation and growth rates of ultrafine atmospheric particles: a review of

Explaining global aerosol number concentrations

D. V. Spracklen et al.

Title Page

Abstract

Introduction

Conclusions

References

Tables

Figures

◀

▶

Back

Close

Full Screen / Esc

Printer-friendly Version

Interactive Discussion



- observations, *J. Aerosol Sci.*, 35, 143–176, 2004. 26380
- Kulmala, M., Lehtinen, K. E. J., and Laaksonen, A.: Cluster activation theory as an explanation of the linear dependence between formation rate of 3 nm particles and sulphuric acid concentration, *Atmos. Chem. Phys.*, 6, 787–793, 2006,
5 <http://www.atmos-chem-phys.net/6/787/2006/>. 26381, 26385
- Kulmala, M., Riipinen, I., Sipilä, M., Manninen, H., Petäjä, Junninen, H., Dal Maso, M., Mor-das, G., Mirme, A., Vana, M., Hirsikko, A., Laakso, L., Harrison, R., Hanson, I., Leung, C., Lehtinen, K., and Kerminen, V.-M.: Toward direct measurement of atmospheric nucleation, *Science*, 318, 89–92, 2007. 26381
- 10 Laakso, L., Laakso, H., Aalto, P. P., Keronen, P., Petäjä, T., Nieminen, T., Pohja, T., Siivola, E., Kulmala, M., Kgabi, N., Molefe, M., Mabaso, D., Phalatse, D., Pienaar, K., and Kerminen, V.-M.: Basic characteristics of atmospheric particles, trace gases and meteorology in a relatively clean Southern African Savannah environment, *Atmos. Chem. Phys.*, 8, 4823–4839, 2008,
15 <http://www.atmos-chem-phys.net/8/4823/2008/>. 26409
- Lucas, D. and Akimoto, H.: Evaluating aerosol nucleation parameterizations in a global atmospheric model, *Geophys. Res. Lett.*, 33, L10808, doi:10.1029/2006GL025672, 2006. 26381
- Mäkelä, J., Aalto, P., Jokinen, V., Pohja, T., Nissinen, A., Palmroth, S., Markkanen, T., Seitsonen, K., Lihavainen, J., and Kulmala, M.: Observations of ultrafine particle formation and growth in boreal forest, *Geophys. Res. Lett.*, 24(10), 1219–1222, 1997. 26380
- 20 Makkonen, R., Asmi, A., Korhonen, H., Kokkola, H., Järvenoja, S., Räisänen, P., Lehtinen, K. E. J., Laaksonen, A., Kerminen, V.-M., Järvinen, H., Lohmann, U., Bennartz, R., Feichter, J., and Kulmala, M.: Sensitivity of aerosol concentrations and cloud properties to nucleation and secondary organic distribution in ECHAM5-HAM global circulation model, *Atmos. Chem. Phys.*, 9, 1747–1766, 2009,
25 <http://www.atmos-chem-phys.net/9/1747/2009/>. 26380, 26382
- Manktelow, P., Mann, G., Carslaw, K., Spracklen, D., and Chipperfield, M.: Regional and global trends in sulfate since the 1980s, *Geophys. Res. Lett.*, 34, L15803, doi:10.1029/2006GL028668, 2007. 26383
- 30 Mårtensson, E., Nilsson, E., de Leeuw, G., Cohen, L., and Hansson, H.: Laboratory simulations and parameterization of the primary marine aerosol production, *J. Geophys. Res.*, 108(D9), 4297, doi:10.1029/2002JD002263, 2003. 26394
- McComiskey, A. E., Andrews, E., Jackson, D., Jefferson, A., Kim, S., Ogren, J., Sheridan, P.,
35 26402

Explaining global aerosol number concentrations

D. V. Spracklen et al.

[Title Page](#)

[Abstract](#)

[Introduction](#)

[Conclusions](#)

[References](#)

[Tables](#)

[Figures](#)

◀

▶

◀

▶

[Back](#)

[Close](#)

[Full Screen / Esc](#)

[Printer-friendly Version](#)

[Interactive Discussion](#)



and Wendell, J.: Aerosols and Radiation, CMDL Summary report,, Tech. Rep. 27, CMDL, 2003. 26409

ACPD

9, 26377–26419, 2009

- McMurtry, P. and Friedlander, S.: New particle formation in the presence of an aerosol, *Atmos. Environ.*, 13, 1635–1651, 1979. 26381
- 5 Merikanto, J., Napari, I., Vehkamäki, H., Antilla, T., and Kulmala, M.: New parameterization of sulfuric acid-ammonia-water ternary nucleation rates at tropospheric conditions, *J. Geophys. Res.*, 11, D15207, doi:10.1029/2006JD007977, 2007. 26381
- Merikanto, J., Spracklen, D. V., Mann, G. W., Pickering, S. J., and Carslaw, K. S.: Impact of nucleation on global CCN, *Atmos. Chem. Phys.*, 9, 8601–8616, 2009,
10 <http://www.atmos-chem-phys.net/9/8601/2009/>. 26396
- Modgil, M., Kumar, S., Tripathi, S., and Lovejoy, E.: A parameterization of ion-induced nucleation of sulfuric acid and water for atmospheric conditions, *J. Geophys. Res.*, 110, D19205, doi:10.1029/2004JD005475, 2005. 26381
- Napari, I., Noppel, M., Vehkamäki, H., and Kulmala, M.: An improved model for ternary
15 nucleation of sulfuric acid-ammonia-water, *J. Chem. Phys.*, 116, 4221–4227, 2002. 26381
- Nightingale, P., Liss, P., and Schlosser, P.: Measurements of air-sea gas transfer during an open ocean algal bloom, *Geophys. Res. Lett.*, 27(14), 2117–2120, 2000. 26384
- O'Dowd, C., Geever, M., Hill, M., Smith, M., and Jennings, S.: New particle formation: Nucleation rates and spatial scales in the clean marine coastal environment, *Geophys. Res. Lett.*,
20 25(10), 1661–1664, 1998. 26409
- O'Dowd, C., Lowe, J., Smith, M., and Kaye, A.: The relative importance of non-sea-salt sulphate and sea-salt aerosol to the marine cloud condensation nuclei population: An improved multi-component aerosol-cloud droplet parametrization, *Q. J. Roy. Meteorol. Soc.*, 125, 1295–1313, 1999. 26380
- 25 O'Dowd, C., Jimenez, J., Bahreini, R., Flagan, R., Seinfeld, J., Hämeri, K., Pirjola, L., Kulmala, M., Jennings, S., and Hoffmann, T.: Marine aerosol formation from biogenic iodine emissions, *Nature*, 417, 632–636, 2002. 26391, 26396
- O'Dowd, C. D., Yoon, Y. J., Junkermann, W., Aalto, P., Kulmala, M., Lihavainen, H., and Viisanen, Y.: Airborne measurements of nucleation mode particles II: boreal forest nucleation events, *Atmos. Chem. Phys.*, 9, 937–944, 2009,
30 <http://www.atmos-chem-phys.net/9/937/2009/>. 26386
- Pierce, J. and Adams, P.: Global evaluation of CCN formation by direct emission of sea salt and growth of ultrafine sea salt, *J. Geophys. Res.*, 111, D06203, doi:10.1029/2005JD006186,

Explaining global aerosol number concentrations

D. V. Spracklen et al.

Title Page

Abstract

Introduction

Conclusions

References

Tables

Figures

◀

▶

◀

▶

Back

Close

Full Screen / Esc

Printer-friendly Version

Interactive Discussion



2006. 26381, 26382, 26393, 26394

Pierce, J., Theodoritsi, G., Adams, P., and Pandis, S. N.: Parameterization of the effect of sub-grid scale aerosol dynamics on aerosol number emission rates, *J. Aerosol Sci.*, 40(5), 385–393, 2009. 26382

5 Pierce, J. R. and Adams, P. J.: Uncertainty in global CCN concentrations from uncertain aerosol nucleation and primary emission rates, *Atmos. Chem. Phys.*, 9, 1339–1356, 2009, <http://www.atmos-chem-phys.net/9/1339/2009/>. 26380, 26382, 26390

10 Pierce, J. R., Chen, K., and Adams, P. J.: Contribution of primary carbonaceous aerosol to cloud condensation nuclei: processes and uncertainties evaluated with a global aerosol microphysics model, *Atmos. Chem. Phys.*, 7, 5447–5466, 2007, <http://www.atmos-chem-phys.net/7/5447/2007/>. 26381, 26382, 26393

Raes, F., Van Dingenen, R., Vignati, E., Wilson, J., Putaud, J.-P., Seinfeld, J., and Adams, P.: Formation and cycling of aerosols in the global troposphere, *Atmos. Environ.*, 34, 4215–4240, 2000. 26387

15 Reade, L., Jennings, S., and McSweeney, G.: Cloud condensation nuclei measurements at Mace Head, Ireland, over the period 1994–2002, *Atmos. Environ.*, 82, 610–621, 2006. 26388

Riipinen, I., Sihto, S.-L., Kulmala, M., Arnold, F., Dal Maso, M., Birmili, W., Saarnio, K., Teinilä, K., Kerminen, V.-M., Laaksonen, A., and Lehtinen, K. E. J.: Connections between atmospheric sulphuric acid and new particle formation during QUEST IIIV campaigns in Heidelberg and Hyytiälä, *Atmos. Chem. Phys.*, 7, 1899–1914, 2007, <http://www.atmos-chem-phys.net/7/1899/2007/>. 26381, 26391, 26395

Schröder, F., Kärcher, B., Fiebig, M., and Petzold, A.: Aerosol states in the free troposphere at northern midlatitudes, *J. Geophys. Res.*, 107(D21), 8126–8133, 2002. 26386

25 Sihto, S.-L., Kulmala, M., Kerminen, V.-M., Dal Maso, M., Petäjä, T., Riipinen, I., Korhonen, H., Arnold, F., Janson, R., Boy, M., Laaksonen, A., and Lehtinen, K. E. J.: Atmospheric sulphuric acid and aerosol formation: implications from atmospheric measurements for nucleation and early growth mechanisms, *Atmos. Chem. Phys.*, 6, 4079–4091, 2006, <http://www.atmos-chem-phys.net/6/4079/2006/>. 26381, 26385

30 Singh, H., Anderson, B., Avery, M., Viezee, W., Chen, Y., Tabazadeh, A., Hamill, P., Pueschel, R., Fuelberg, H., and Hannan, J.: Global distribution and sources of volatile and nonvolatile aerosol in the remote troposphere, *J. Geophys. Res.*, 107(D11), 4121, doi:10.1029/2001JD000486, 2002. 26386

Spracklen, D., Carslaw, K., Kulmala, M., Kerminen, V.-M., Sihto, S.-L., Riipinen, I., Merikanto, J.,

Explaining global aerosol number concentrations

D. V. Spracklen et al.

Title Page

Abstract

Introduction

Conclusions

References

Tables

Figures

◀

▶

◀

▶

Back

Close

Full Screen / Esc

Printer-friendly Version

Interactive Discussion



- Mann, G., Chipperfield, M., Wiedensohler, A., Birmili, W., and Lihavainen, H.: Contribution of particle formation to global cloud condensation nuclei concentrations, *Geophys. Res. Lett.*, 35, L06808, doi:10.1029/2007GL033038, 2008. 26380, 26382, 26383, 26386
- Spracklen, D. V., Pringle, K. J., Carslaw, K. S., Chipperfield, M. P., and Mann, G. W.: A global off-line model of size-resolved aerosol microphysics: I. Model development and prediction of aerosol properties, *Atmos. Chem. Phys.*, 5, 2227–2252, 2005,
<http://www.atmos-chem-phys.net/5/2227/2005/>. 26381, 26382, 26383, 26384, 26393
- Spracklen, D. V., Pringle, K. J., Carslaw, K. S., Chipperfield, M. P., and Mann, G. W.: A global off-line model of size-resolved aerosol microphysics: II. Identification of key uncertainties, *Atmos. Chem. Phys.*, 5, 3233–3250, 2005,
<http://www.atmos-chem-phys.net/5/3233/2005/>. 26380, 26381, 26382, 26383, 26387, 26393
- Spracklen, D. V., Carslaw, K. S., Kulmala, M., Kerminen, V.-M., Mann, G. W., and Sihto, S.-L.: The contribution of boundary layer nucleation events to total particle concentrations on regional and global scales, *Atmos. Chem. Phys.*, 6, 5631–5648, 2006,
<http://www.atmos-chem-phys.net/6/5631/2006/>. 26380, 26382, 26384, 26386
- Spracklen, D. V., Pringle, K. J., Carslaw, K. S., Mann, G. W., Manktelow, P., and Heintzenberg, J.: Evaluation of a global aerosol microphysics model against size-resolved particle statistics in the marine atmosphere, *Atmos. Chem. Phys.*, 7, 2073–2090, 2007,
<http://www.atmos-chem-phys.net/7/2073/2007/>. 26382
- Stier, P., Feichter, J., Kinne, S., Kloster, S., Vignati, E., Wilson, J., Ganzeveld, L., Tegen, I., Werner, M., Balkanski, Y., Schulz, M., Boucher, O., Minikin, A., and Petzold, A.: The aerosol-climate model ECHAM5-HAM, *Atmos. Chem. Phys.*, 5, 1125–1156, 2005,
<http://www.atmos-chem-phys.net/5/1125/2005/>. 26381, 26384, 26385, 26408
- Trivitayanurak, W., Adams, P. J., Spracklen, D. V., and Carslaw, K. S.: Tropospheric aerosol microphysics simulation with assimilated meteorology: model description and intermodel comparison, *Atmos. Chem. Phys.*, 8, 3149–3168, 2008,
<http://www.atmos-chem-phys.net/8/3149/2008/>. 26382, 26393
- Vana, M., Kulmala, M., Maso, D., Hörrak, M., and Tamm, E.: Comparative study of nucleation mode aerosol particles and intermediate air ions formation events at three sites, *J. Geophys. Res.*, 109(D17), D17201, doi:10.1029/2003JD004413, 2004. 26380
- Vehkamäki, H., Kulmala, M., Napari, I., Lehtinen, K., Timmreck, C., Noppel, M., and Laaksonen, A.: An improved parametrization for sulfuric acid-water nucleation rates for tropospheric and stratospheric conditions, *J. Geophys. Res.*, 107(22), 4622–4631, 2002. 26381

Title Page	
Abstract	Introduction
Conclusions	References
Tables	Figures
	
	
Back	Close
Full Screen / Esc	
Printer-friendly Version	
Interactive Discussion	



- Vehkamäki, H., Napari, I., Kulmala, M., and Noppel, M.: Stable ammonium bisulfate clusters in the atmosphere, *Phys. Rev. Lett.*, 93(14), 148501, doi:10.1103/PhysRevLett.93.14850, 2004. 26380
- Venzac, H., Sellegri, K., Laj, P., Villani, P., Bonasoni, P., Marinoni, A., Cristofanelli, P., Calzolari, F., Fuzzi, S., Decesari, S., Facchini, M.-C., Vuillermoz, E., and Verza, G. P.: High frequency new particle formation in the Himilayas, *P. Natl. Acad. Sci. USA*, 105, 15666–15671, 2008. 26380, 26409
- Venzac, H., Sellegri, K., Villani, P., Picard, D., and Laj, P.: Seasonal variation of aerosol size distributions in the free troposphere and residual layer at the puy de Dôme station, France, *Atmos. Chem. Phys.*, 9, 1465–1478, 2009,
<http://www.atmos-chem-phys.net/9/1465/2009/>. 26388, 26409
- Verheggen, B., Mozurkewich, M., Caffrey, P., Hoppel, W., and Sullivan, W.: Alpha-pinene oxidation in the presence of seed aerosol: Estimates of nucleation rates, growth rates, and yield, *Environ. Sci. Technol.*, 41(17), 6046–6051, 2007. 26391
- Vuollekoski, H., Kerminen, V.-M., Anttila, T., Sihto, S.-L., Vana, M., Ehn, M., Korhonen, H., McFiggans, G., O'Dowd, C. D., and Kulmala, M.: Iodine dioxide nucleation simulations in coastal and remote marine environments, *J. Geophys. Res.*, 114, D02206, doi:10.1029/2008JD010713, 2009. 26396
- Wang, M. and Penner, J. E.: Aerosol indirect forcing in a global model with particle nucleation, *Atmos. Chem. Phys.*, 9, 239–260, 2009,
<http://www.atmos-chem-phys.net/9/239/2009/>. . 26380
- Wang, M., Penner, J., and Liu, X.: The coupled IMPACT aerosol and NCAR CAM3 model: Evaluation of predicted aerosol number and size distribution, *J. Geophys. Res.*, 114, D06302, doi:10.1029/2008JD010459, 2009. 26382, 26393
- Weber, R., Marti, J., McMurry, P., Eisele, F., Tanner, D., and Jefferson, A.: Measured atmospheric new particle formation rates: Implications for nucleation mechanisms, *Chem. Eng. Commun.*, 151, 53–64, 1996. 26381
- Weber, R., McMurry, P., Mauldin III, R., Tanner, D., Eisele, F., Clarke, A., and Kapustin, V.: New particle formation in the remote troposphere: A comparison of observations at various sites, *Geophys. Res. Lett.*, 26(3), 307–310, 1999. 26381
- Weingartner, E., Nyeki, S., and Baltensperger, U.: Seasonal and diurnal variation of aerosol size distributions ($10 < D < 750 \text{ nm}$) at a high-alpine site (Jungfraujoch 3580 m a.s.l.), *J. Geophys. Res.*, 104(D21), 26809–26820, 1999. 26380, 26409

Explaining global aerosol number concentrations

D. V. Spracklen et al.

[Title Page](#)

[Abstract](#)

[Introduction](#)

[Conclusions](#)

[References](#)

[Tables](#)

[Figures](#)

◀

▶

◀

▶

[Back](#)

[Close](#)

[Full Screen / Esc](#)

[Printer-friendly Version](#)

[Interactive Discussion](#)



- Weller, R. and Lampert, A.: Optical properties and sulfate scattering efficiency of boundary layer aerosol at coastal Neumayer Station, *J. Geophys. Res.*, 113, D16208, doi:10.1029/2008JD009962, 2008. 26409
- 5 Yu, F.: Effect of ammonia on new particle formation: a kinetic $\text{H}_2\text{SO}_4\text{-H}_2\text{O-NH}_3$ nucleation model constrained by laboratory measurements, *J. Geophys. Res.*, 111, D01204, doi:10.1029/2005JD005968, 2006. 26381
- Yu, F., Wang, Z., Luo, G., and Turco, R.: Ion-mediated nucleation as an important global source of tropospheric aerosols, *Atmos. Chem. Phys.*, 8, 2537–2554, 2008,
<http://www.atmos-chem-phys.net/8/2537/2008/>. 26381
- 10 Ziembba, L., Griffin, R., and Talbot, R.: Observations of elevated particle number concentration events at a rural site in New England, *J. Geophys. Res.*, 111, D23S34, doi:10.1029/2006JD007607, 2007. 26409

Explaining global aerosol number concentrations

D. V. Spracklen et al.

[Title Page](#)

[Abstract](#)

[Introduction](#)

[Conclusions](#)

[References](#)

[Tables](#)

[Figures](#)

◀

▶

◀

▶

[Back](#)

[Close](#)

[Full Screen / Esc](#)

[Printer-friendly Version](#)

[Interactive Discussion](#)



Explaining global aerosol number concentrations

D. V. Spracklen et al.

Table 1. Simulated annual mean (median) surface CN ($D_p > 3 \text{ nm}$) concentrations (at ambient temperature and pressure) for the year 2000 for model experiments with different primary emissions and particle formation (see Sect. 2.2 for details).

Experiment Name	Size distribution of primary emissions		Nucleation mechanisms	Surface mean (median) CN	
	EC/OC	Sulfate		Ocean/cm ⁻³	Land/cm ⁻³
PRI	Stier et al. (2005)	AEROCOM	None	105 (30)	642 (107)
BHN	Stier et al. (2005)	AEROCOM	BHN	352 (252)	952 (604)
PRICAR	AEROCOM	AEROCOM	BHN	495 (265)	2230 (839)
PRISUL	Stier et al. (2005)	Adams and Seinfeld (2003)	BHN	595 (267)	2282 (721)
ACT1	Stier et al. (2005)	AEROCOM	BHN + Activation ($A=2\times 10^{-7} \text{ s}^{-1}$)	474 (323)	1262 (703)
ACT2	Stier et al. (2005)	AEROCOM	BHN + Activation ($A=2\times 10^{-6} \text{ s}^{-1}$)	729 (483)	1743 (868)
ACT3	Stier et al. (2005)	AEROCOM	BHN + Activation ($A=2\times 10^{-5} \text{ s}^{-1}$)	1157 (660)	2653 (1018)
KIN1	Stier et al. (2005)	AEROCOM	BHN + Kinetic ($A=2\times 10^{-13} \text{ cm}^3 \text{ s}^{-1}$)	557 (323)	1498 (725)
KIN2	Stier et al. (2005)	AEROCOM	BHN + Kinetic ($A=2\times 10^{-12} \text{ cm}^3 \text{ s}^{-1}$)	798 (426)	2003 (813)
KIN3	Stier et al. (2005)	AEROCOM	BHN + Kinetic ($A=2\times 10^{-11} \text{ cm}^3 \text{ s}^{-1}$)	1181 (550)	2764 (878)

- [Title Page](#)
- [Abstract](#) [Introduction](#)
- [Conclusions](#) [References](#)
- [Tables](#) [Figures](#)
- [◀](#) [▶](#)
- [◀](#) [▶](#)
- [Back](#) [Close](#)
- [Full Screen / Esc](#)
- [Printer-friendly Version](#)
- [Interactive Discussion](#)



Table 2. Observation sites used in this analysis.

Station Name	Location	Altitude (m)	Observation period	Minimum cutoff diameter (nm)	Data source ¹	Reference
Free troposphere						
Jungfraujoch	8.0° E, 46.6° N	3580	1995–1999, 2003–2007	10	E	Weingartner et al. (1999)
Puy de Dome	3.0° E, 45.8° N	1465	2005–2008	3	E	Venzac et al. (2009)
Nepal C.O.	86.8° E, 28.0° N	5079	2007–2008	10	P	Venzac et al. (2008)
Mauna Loa	155.6° W, 19.5° N	3397	1975–2000	14	W	Bodhaine (1983)
South Pole	24.8° W, 90° S	2841	1974–1999	14	W	Bodhaine (1983)
Pico Espejo	71.1° W, 8.5° N	4775	2007–2009	10	P	
Mount Washington	71.3° W, 44.3° N	1910	2002–2005	10	A	
Mount Waliguan	100.9° E, 36.3° N	3816	2005–2007	13	P	Kivekäs et al. (2009)
Zugspitze	11.0° E, 47.4° N	2650	2005–2008	12	P	
Marine boundary layer						
Mace Head	9.9° W, 53.3° N	5	2000, 2002–2007	10	E	O'Dowd et al. (1998)
Neumayer	8.3° W, 70.7° S	42	1993–2006	14	W	Weller and Lampert (2008)
Point Barrow	156.6° W, 71.3° N	11	1994–2007	14	W	Delene and Ogren (2002)
Samoa	170.6° W, 14.2° S	77	1977–2006	14	W	Bodhaine (1983)
Trinidad Head	124.2° W, 41.1° N	107	2002–2007	14	W	McComiskey et al. (2003)
Cape Grim	144.7° E, 40.6° S	94	1996–2007	3	W	Gras (1995)
Sable Island	60.0° W, 43.9° N	5	1992–2000	10	P	Delene and Ogren (2002)
Continental boundary layer						
Hyytiälä	24.3° E, 61.9° N	180	2000–2004	3	C	Aalto et al. (2001)
Pallas	24.1° E, 68.0° N	340	2000–2004, 2007	10	E	Komppula et al. (2003)
Finokalia	25.7° E, 35.3° N	250	1997, 2006–2007	10	E	
Hohenpeissenberg	11.0° E, 47.8° N	995	2006–2007	3	E	Birmili et al. (2003)
Melpitz	12.3° E, 51.2° N	86	1996–1997, 2003	3	C	
Bondville	88.4° W, 40.1° N	213	1994–2007	14	W	Delene and Ogren (2002)
Southern Great Plains	97.5° W, 36.6° N	320	1996–2007	10	W	Delene and Ogren (2002)
Tomsk	85.1° E, 56.5° N	170	2005–2006	3	PD	Dal Maso et al. (2008b)
Listvyanka	104.9° E, 51.9° N	750	2005–2006	3	PD	Dal Maso et al. (2008b)
Harwell	359.0° E, 51.0° N	60	2000	10	U	Charron et al. (2007)
Weybourne	1.1° E, 53.0° N	0	2005	10	B	
Botsalano	25.8° E, 25.5° S	1424	7/2006–6/2007	10	PD	Laakso et al. (2008)
India Himalaya	79.6° E, 29.4° N	2180	2005–2008	10	PD	Komppula et al. (2009)
Aspvreten	17.4° E, 58.8° N	25	2000–2006	10	PD	Dal Maso et al. (2008a)
Utö	21.4° E, 59.8° N	8	2003–2006	7	PD	Dal Maso et al. (2008a)
Värriö	29.6° E, 67.8° N	400	1998–2006	8	PD	Dal Maso et al. (2008a)
Thompson Farm	289.1° E, 43.1° N	75	2001–2009	7	A	Ziembra et al. (2007)
Castle Springs	71.3° W, 43.7° N	406	2001–2008	7	A	
Tannus Observatory	8.4° E, 50.2° N	810	2008–2009	10	P	
Po Valley	11.6° W, 44.7° N	11	2002–2006	3	P	Hamed et al. (2007)

¹ AIRMAP, <http://airmap.unh.edu/data/> (A); BADC, <http://badc.nerc.ac.uk/home/> (B); CREATE, <http://tarantula.nilu.no/projects/ccc/create/> (C); EBAS, <http://ebas.nilu.no> (E); Personal communication (P); Published data, see citation (PD); UK National Air Quality Archive, <http://www.airquality.co.uk/> (U); World Data Centre for Aerosols (WDCA), <http://wdca.jrc.ec.europa.eu/> (W).

Explaining global aerosol number concentrations

D. V. Spracklen et al.

[Title Page](#)

[Abstract](#)

[Introduction](#)

[Conclusions](#)

[References](#)

[Tables](#)

[Figures](#)



[Back](#)

[Close](#)

[Full Screen / Esc](#)

[Printer-friendly Version](#)

[Interactive Discussion](#)



Explaining global aerosol number concentrations

D. V. Spracklen et al.

Table 3. Normalised mean bias between observed and simulated CN concentrations. Model experiments are described in Table 1, locations and time periods of the observations are shown in Table 2.

Stations	Model experiments									
	PRI	BHN	PRICAR	PRISUL	ACT1	ACT2	ACT3	KIN1	KIN2	KIN3
All	-76%	-62%	-12%	37%	-44%	-24%	17%	-31%	-9%	35%
FT	-88%	-25%	-6%	-18%	-9%	14%	53%	5%	28%	68%
MBL	-85%	-61%	-28%	11%	-40%	-12%	23%	-27%	-3%	21%
BL	-74%	-66%	-15%	46%	-48%	-29%	12%	-35%	-13%	31%



Table 4. Correlation coefficient (R^2) between observed and simulated monthly mean CN concentrations at sites where monthly mean concentrations vary by more than a factor of two throughout a seasonal cycle. Model experiments are described in Table 1.

Site	PRI	BHN	PRICAR	PRISUL	ACT2	KIN2
Free troposphere						
Puy de Dome	0.01	0.01	0.05	0.07	0.19	0.06
Nepal C.O.	0.01	0.01	<0.01	0.11	0.18	0.37
South Pole	0.08	0.65	0.44	0.69	0.71	0.72
Mt. Washington	0.25	0.38	0.01	0.02	0.02	0.29
Marine boundary layer						
Neumayer	0.02	0.74	0.57	0.62	0.71	0.68
Point Barrow	0.04	0.03	0.06	0.02	0.07	0.04
Sable Island	0.37	0.31	<0.01	0.43	0.25	0.57
Continental boundary layer						
Hyytiälä	0.13	0.01	0.06	0.26	0.39	0.43
Pallas	0.12	0.19	0.07	0.25	0.55	0.59
Melpitz	0.06	0.02	0.05	0.07	0.28	0.41
Tomsk	0.14	0.05	0.26	<0.01	0.04	<0.01
Listvyanka	0.09	0.05	0.20	<0.01	0.13	0.07
Harwell	0.25	0.10	0.12	0.33	0.40	0.48
Weybourne	<0.01	0.08	0.03	0.02	0.05	0.03
India Himalaya	0.18	0.40	0.25	0.61	<0.01	0.01
Utö	0.08	0.03	0.26	0.10	0.10	0.30
Väriö	0.03	<0.01	<0.01	0.06	0.56	0.65
Tannus	0.21	0.14	0.27	0.25	0.21	0.29

Explaining global aerosol number concentrations

D. V. Spracklen et al.

[Title Page](#)

[Abstract](#)

[Introduction](#)

[Conclusions](#)

[References](#)

[Tables](#)

[Figures](#)

◀

▶

◀

▶

[Back](#)

[Close](#)

[Full Screen / Esc](#)

[Printer-friendly Version](#)

[Interactive Discussion](#)



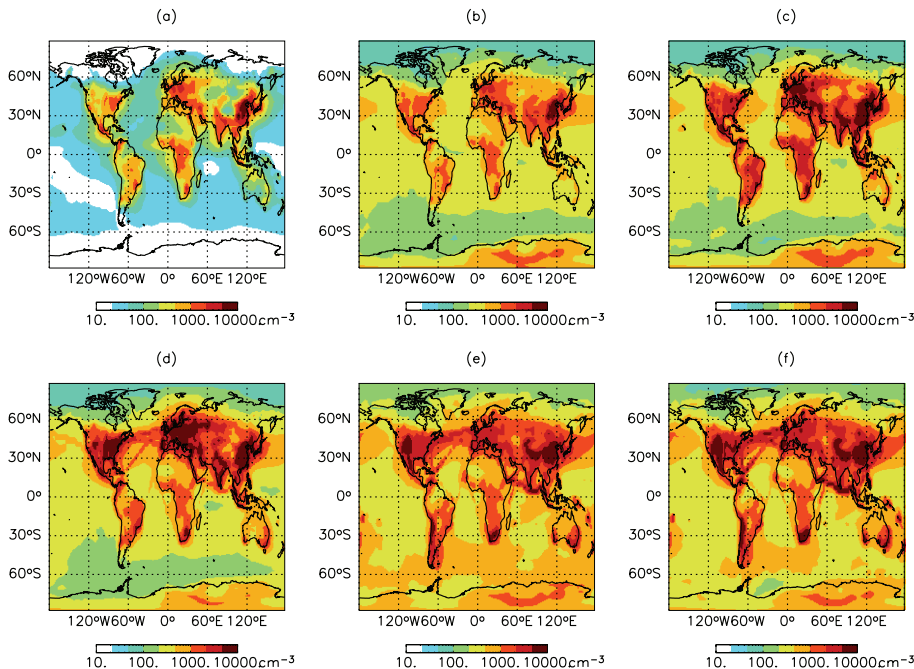


Fig. 1. Simulated surface annual mean CN ($D_p > 3 \text{ nm}$) concentrations (at ambient temperature and pressure) for the different experiments described in Table 1: **(a)** Primary emissions only (PRI), **(b)** Primary emissions and binary homogeneous nucleation (BHN), **(c)** BHN and increased primary EC/OC (PRICAR), **(d)** BHN and increased primary sulfate (PRISUL), **(e)** Primary emissions, BHN and activation particle formation (ACT2), **(f)** Primary emissions, BHN and kinetic particle formation (KIN2).

Explaining global aerosol number concentrations

D. V. Spracklen et al.

[Title Page](#)

[Abstract](#)

[Introduction](#)

[Conclusions](#)

[References](#)

[Tables](#)

[Figures](#)



[Back](#)

[Close](#)

[Full Screen / Esc](#)

[Printer-friendly Version](#)

[Interactive Discussion](#)

Explaining global aerosol number concentrations

D. V. Spracklen et al.

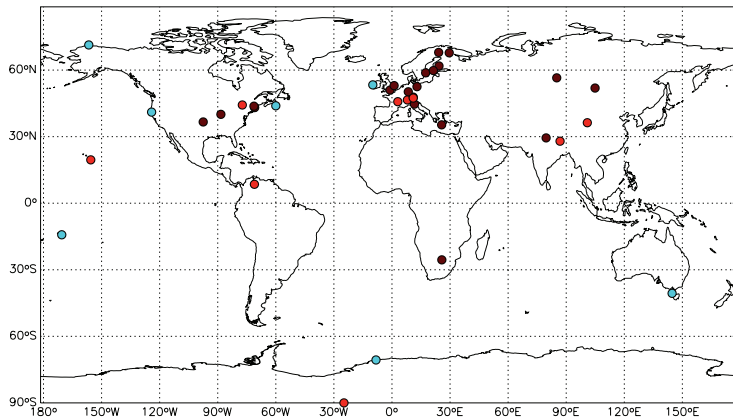


Fig. 2. Location of observation sites used in this analysis classified as in Table 2: FT (red), MBL (blue), continental BL (brown).

[Title Page](#)

[Abstract](#)

[Introduction](#)

[Conclusions](#)

[References](#)

[Tables](#)

[Figures](#)

◀

▶

◀

▶

[Back](#)

[Close](#)

[Full Screen / Esc](#)

[Printer-friendly Version](#)

[Interactive Discussion](#)



Explaining global aerosol number concentrations

D. V. Spracklen et al.

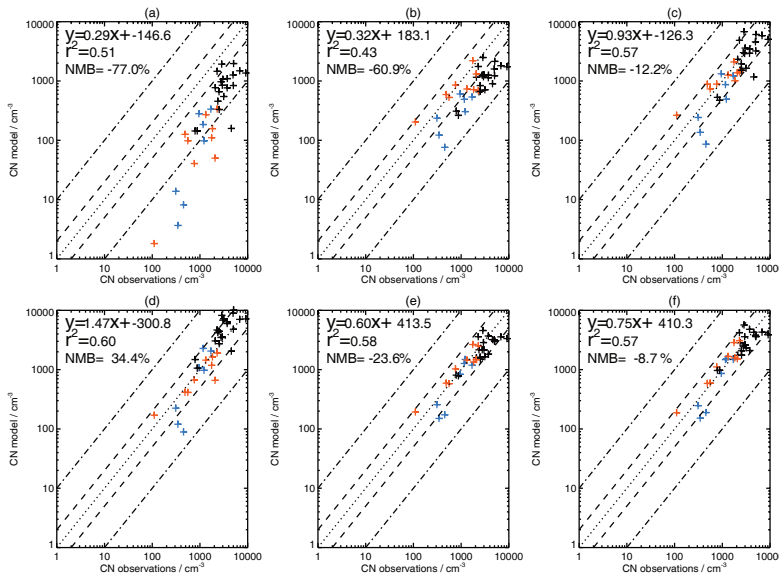


Fig. 3. Scatterplot of simulated (GLOMAP) versus observed annual mean CN concentrations (at ambient temperature and pressure) for the sites shown in Fig. 2. Sites are classified as FT (red), MBL (blue) and continental BL (black) as shown in Table 2. The different model experiments are described in Table 1: **(a)** Primary emissions only (PRI), **(b)** Primary emissions and binary homogeneous nucleation (BHN), **(c)** BHN and increased primary EC/OC (PRICAR), **(d)** BHN and increased primary sulfate (PRISUL), **(e)** Primary emissions, BHN and activation particle formation (ACT2), **(f)** Primary emissions, BHN and kinetic particle formation (KIN2). The regression equation for the reduced major axis linear regression, Pearson correlation coefficients (R^2) and normalised mean bias (NMB) are shown. The dotted line represents the 1:1 relation and the dashed lines factor of 2 and 10 deviations.

Explaining global aerosol number concentrations

D. V. Spracklen et al.

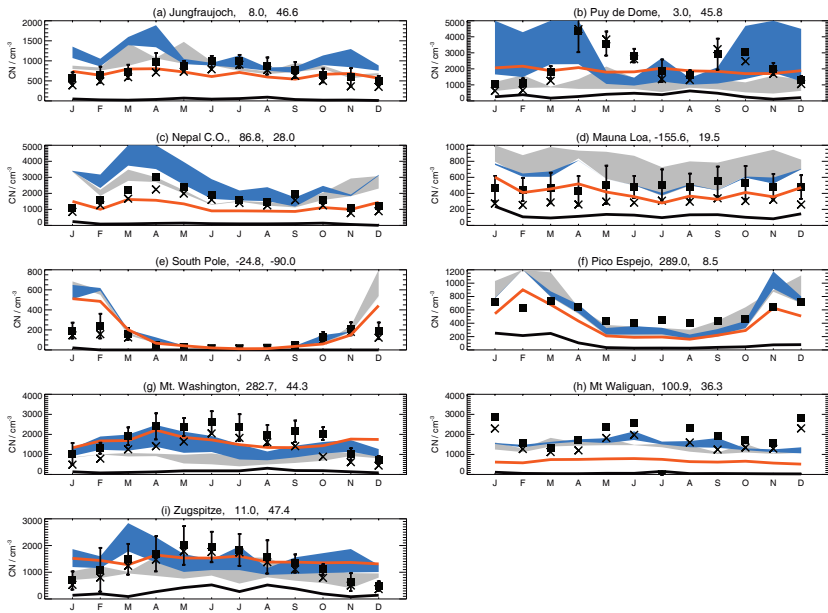


Fig. 4. Seasonal cycle of CN concentrations (at ambient temperature and pressure) at the FT sites shown in Table 2. Solid squares show observed monthly mean concentrations, crosses show observed monthly median concentrations and vertical bars show the standard deviation of the observed monthly mean (displayed only where there are 4 or more years of observations). The model experiments are described in Table 1: Black line shows the model with primary particulate emissions only (PRI), bottom of grey shading shows model with primary emissions and BHN (BHN), top of grey shading shows model with BHN and increased EC/OC number emission (PRICAR). Red line shows model with BHN and increased primary sulfate number emission (PRISUL). Blue shading shows model with primary emissions, BHN and activation BL particle formation, with the width of shading showing sensitivity to varying nucleation coefficients from $A=2\times10^{-7}\text{ s}^{-1}$ (ACT1) to $A=2\times10^{-5}\text{ s}^{-1}$ (ACT3).

Title Page

Abstract

Introduction

Conclusions

References

Tables

Figures



Back

Close

Full Screen / Esc

Printer-friendly Version

Interactive Discussion

Explaining global aerosol number concentrations

D. V. Spracklen et al.

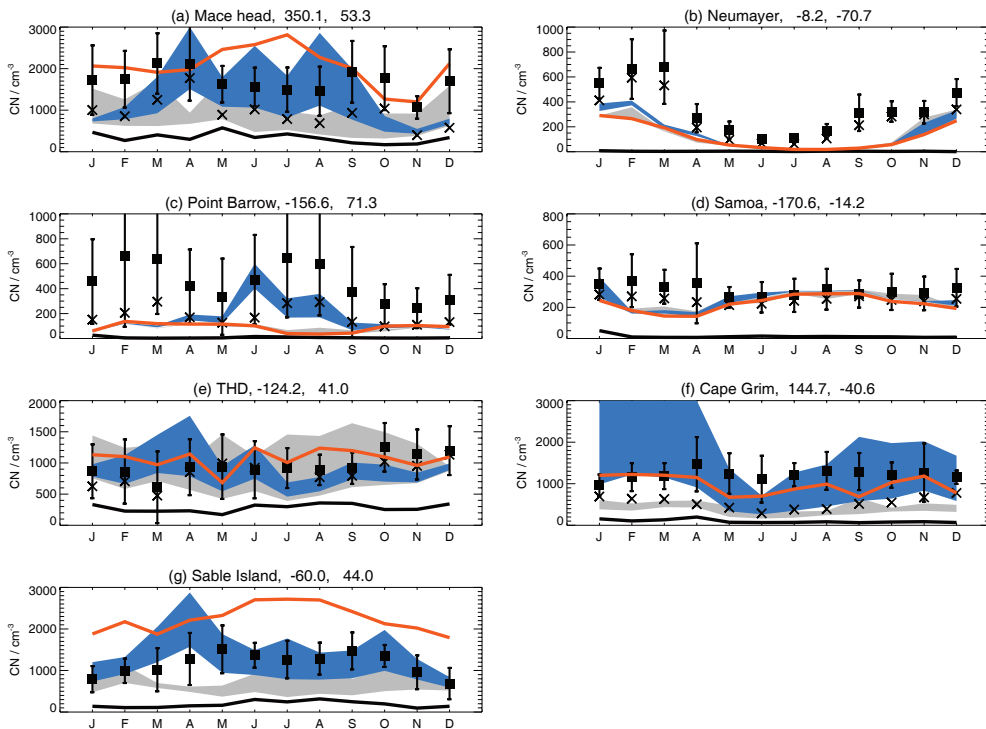


Fig. 5. As for Fig. 4 but for MBL sites.



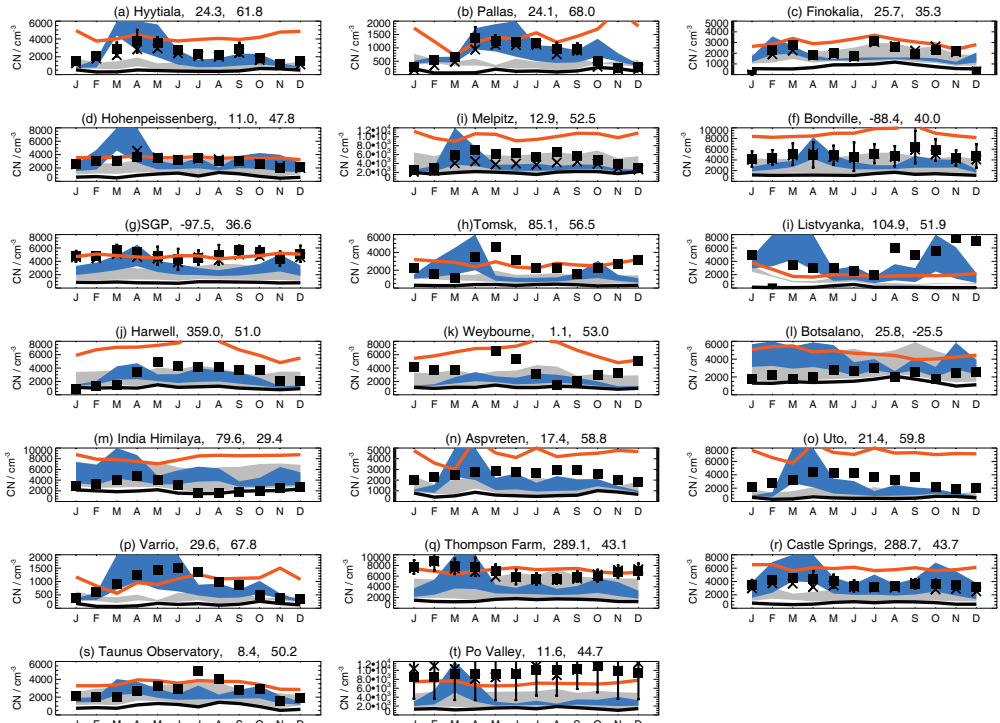


Fig. 6. As for Fig. 4 but for BL sites.

Explaining global aerosol number concentrations

D. V. Spracklen et al.

[Title Page](#)

[Abstract](#)

[Introduction](#)

[Conclusions](#)

[References](#)

[Tables](#)

[Figures](#)



[Full Screen / Esc](#)

[Printer-friendly Version](#)

[Interactive Discussion](#)

Explaining global aerosol number concentrations

D. V. Spracklen et al.

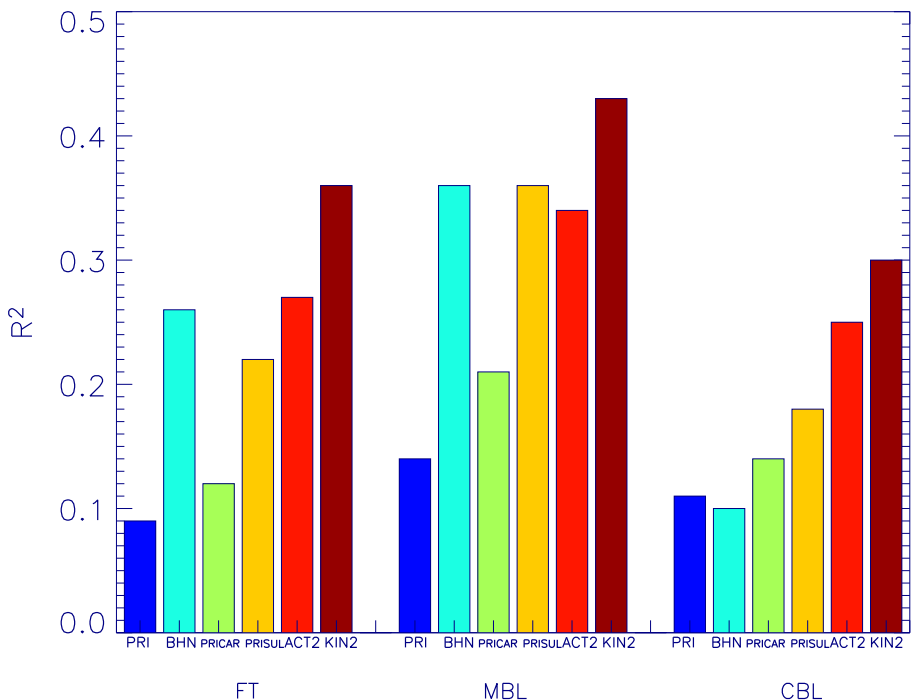


Fig. 7. Correlation coefficients (R^2) between simulated and observed monthly mean CN concentrations calculated for the FT, MBL and continental BL (CBL) sites in Table 4. Model runs are described in Table 1.

Title Page	
Abstract	Introduction
Conclusions	References
Tables	Figures
◀	▶
◀	▶
Back	Close
Full Screen / Esc	
Printer-friendly Version	
Interactive Discussion	

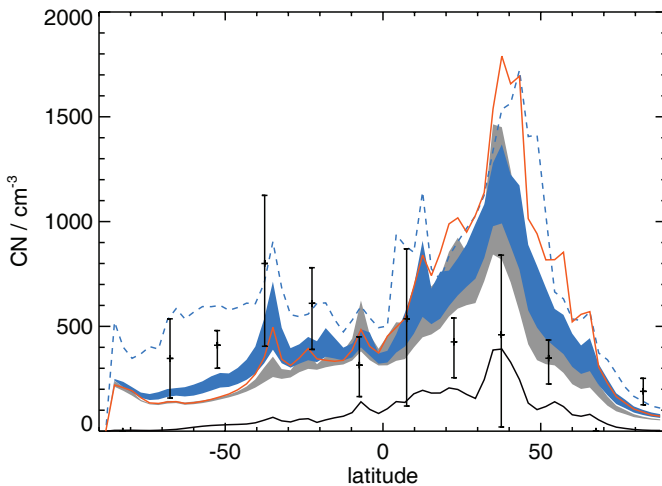


Fig. 8. Annual mean surface CN concentrations over the global oceans versus latitude. Observations (vertical bars) have been compiled from several field campaigns (Heintzenberg et al., 2000) and show mean concentrations \pm one standard deviation. The model experiments are described in Table 1: Black line shows the model with primary particulate emissions only (PRI), bottom of grey shading shows model with primary emissions and BHN (BHN), top of grey shading shows model with BHN and increased EC/OC number emission (PRICAR). Red line shows model with BHN and increased primary sulfate number emission (PRISUL). Blue shading shows model with primary emissions, BHN and activation BL particle formation, with the width of shading showing sensitivity to varying nucleation coefficients from $A=2\times10^{-7}\text{ s}^{-1}$ (ACT1) to $A=2\times10^{-5}\text{ s}^{-1}$ (ACT3). All model experiments are for CN ($>12\text{ nm}$) except the blue dashed line which shows CN ($>3\text{ nm}$) for the ACT2 simulation.

Explaining global aerosol number concentrations

D. V. Spracklen et al.

[Title Page](#)

[Abstract](#)

[Introduction](#)

[Conclusions](#)

[References](#)

[Tables](#)

[Figures](#)

◀

▶

[Back](#)

[Close](#)

[Full Screen / Esc](#)

[Printer-friendly Version](#)

[Interactive Discussion](#)

